

## 5. EXPLANATORY NOTES<sup>1</sup>

### Shipboard Scientific Party<sup>2</sup>

In this chapter, we have assembled information that will help the reader understand the basis for our preliminary conclusions and also help the interested investigator select samples for further analysis. This information concerns only shipboard operations and analyses described in the site reports in the *Initial Reports* volume of the Leg 143 *Proceedings of the Ocean Drilling Program*. Methods used by various investigators for shore-based analysis of Leg 143 data will be detailed in the individual scientific contributions published in the *Scientific Results* volume.

#### Authorship of Site Chapters

The separate sections of the site chapters were written by the following shipboard scientists (authors are listed in alphabetical order, no seniority is necessarily implied):

Site Summary: Sager, Winterer  
Background and Scientific Objectives: Sager, Winterer  
Operations: Pollard, Sager, Winterer  
Site Geophysics: Sager, Winterer  
Lithostratigraphy: Arnaud, Flood, Iryu, Jenkyns, Murdmaa, Strasser, Swinburne, van Waasbergen  
Biostratigraphy: Bralower, Firth, Mutterlose, Sliter, Swinburne  
Paleomagnetism: Polgreen, Tarduno  
Sedimentation Rates: Bralower, Firth, Mutterlose,  
Inorganic Geochemistry: Paull, Röhl  
Organic Geochemistry: Baudin  
Physical Properties: Ivanov, Kenter  
Downhole Measurements: Cooper, Golovchenko, Nogi  
Seismic Stratigraphy: Sager, Winterer

Following the site chapters are summary core descriptions ("barrel sheets" and basement rock visual core descriptions) and photographs of each core. In addition, a CD-ROM has been provided (back pocket) that contains 500 Mb of depth-shifted and processed logging data collected during Leg 143. Processing and production of this CD-ROM were done for ODP by the Borehole Research Group at Lamont-Doherty Geological Observatory.

#### Survey and Drilling Data

Geophysical survey data collected during Leg 143 consists of magnetic, bathymetric, and seismic data acquired during the transit from Honolulu to Allison Guyot, from Annewetak Atoll to Majuro, and data collected between sites. These are discussed in the "Underway Geophysics" chapter (this volume), along with a brief description of all geophysical instrumentation and acquisition systems used and a summary listing of Leg 143 navigation. The survey data used for final site selection, including both data collected during site surveys prior to Leg 143 and during short site-location surveys during Leg 143, are presented in the "Site Geophysics" section of the individual site chapters (this volume). During the Leg 143 *JOIDES Resolution*

surveys, single-channel seismic, 3.5- and 12-kHz echo sounder, and magnetic data were recorded across the planned drilling sites to aid site confirmation prior to dropping a beacon.

The single-channel seismic profiling system used either two 80-in.<sup>3</sup> water guns or a 200-in.<sup>3</sup> water gun as the energy source and a Teledyne streamer with a 100-m-long active section. At several sites, one or two 200-in.<sup>3</sup> guns were used as sources for sonobuoy seismic refraction shooting. All seismic data were recorded digitally on tape using a Masscomp 561 super minicomputer and were also displayed in real time in analog format on Raytheon electrostatic recorders using a variety of filter settings and scales.

Bathymetric data collected using the 3.5- and 12-kHz precision depth recorder (PDR) system were each displayed on Raytheon recorders. The depths were calculated on the basis of an assumed 1500-m/s sound velocity in water. The water depth (in meters) at each site was corrected for (1) the variation in sound velocity with depth using Matthews' (1939) tables and (2) the depth of the transducer pod (6.8 m) below sea level. In addition, depths referred to the drilling-platform level have been corrected for the height of the rig floor above the water line, which gradually increased throughout the cruise (see Fig. 1).

Magnetic data collected using a Geometrics 801 proton precession magnetometer were displayed on a strip chart recorder, and were recorded on magnetic tape for later processing.

#### Drilling Characteristics

Because water circulation downhole is open, cuttings are lost onto the seafloor and cannot be examined. The only available information about sedimentary stratification in uncored or unrecovered intervals, other than from seismic data or wireline logging results, is from an examination of the behavior of the drill string as observed and recorded on the drilling platform. Typically, the harder a layer, the slower and more difficult it is to penetrate. A number of other factors may determine the rate of penetration; thus it is not always possible to relate drilling time directly to the hardness of the layers. Bit weight and revolutions per minute, recorded on the drilling recorder, also influence the penetration rate.

#### Drilling Deformation

When cores are split, many show signs of significant sediment disturbance, including the downward-concave appearance of originally horizontal bands, haphazard mixing of lumps of different lithologies (mainly at the tops of cores), and the near-fluid state of some sediments recovered from tens to hundreds of meters below the seafloor. Core deformation probably occurs during cutting, retrieval (with accompanying changes in pressure and temperature), and core handling on deck.

#### Shipboard Scientific Procedures

##### Numbering of Sites, Holes, Cores, and Samples

Drilling sites are numbered consecutively from the first site drilled by the *Glomar Challenger* in 1968. A site number refers to one or more holes drilled while the ship was positioned over one acoustic beacon. Multiple holes may be drilled at a single site by pulling the drill pipe above the seafloor (out of the hole), moving the ship some distance

<sup>1</sup> Sager, W.W., Winterer, E.L., Firth, J.V., et al., 1993. *Proc. ODP, Init. Repts.*, 143: College Station, TX (Ocean Drilling Program).

<sup>2</sup> Shipboard Scientific Party is as given in list of participants preceding the contents.

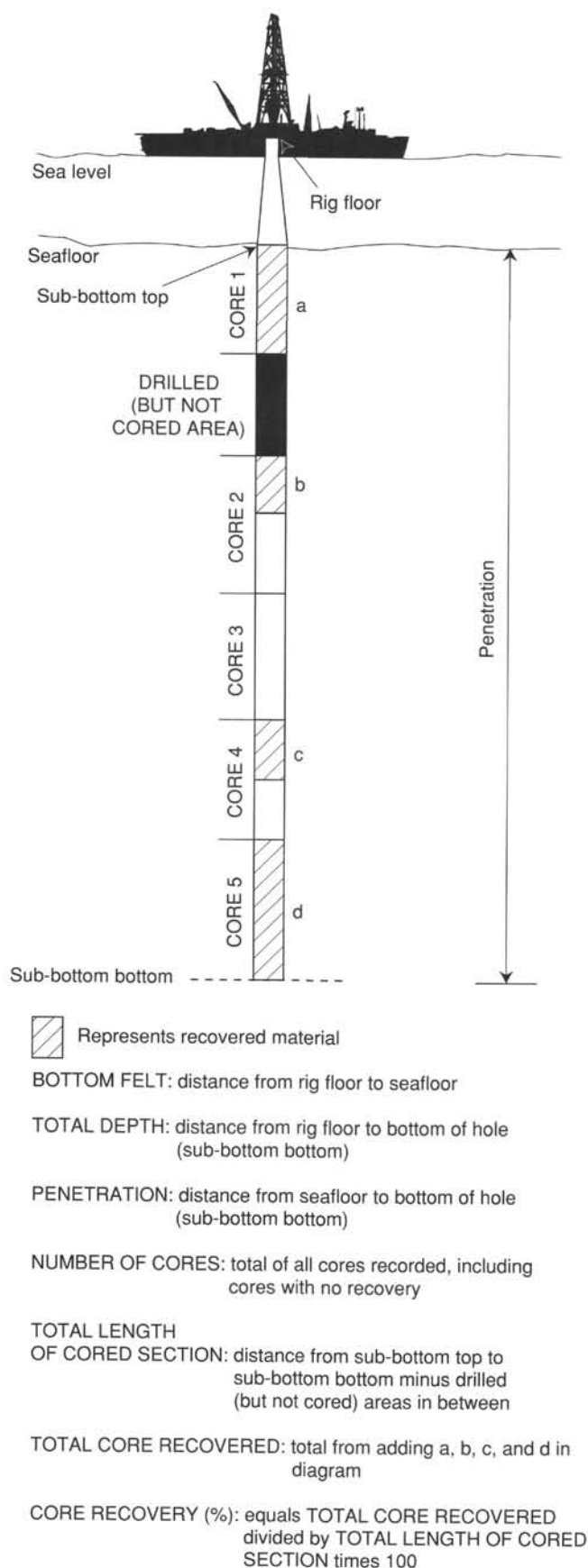


Figure 1. Diagram illustrating terms used in discussion of coring operations and core recovery.

from the previous hole, and then drilling another hole. In some cases, the ship may return to a previously occupied site to drill additional holes.

For all ODP drill sites, a letter suffix distinguishes each hole drilled at the same site. For example, the first hole drilled is assigned the site number modified by the suffix A, the second hole takes the site number and suffix B, and so forth. Note that this procedure differs slightly from that used by DSDP (Sites 1 through 624), but prevents ambiguity between site- and hole-number designations. For sampling purposes, it is important to distinguish among holes drilled at a site. Sediments or rocks recovered from different holes usually do not come from equivalent positions in the stratigraphic column, even if the core numbers are identical.

The cored interval is measured in meters below seafloor (mbsf); sub-bottom depths are determined by subtracting the drill-pipe-measurement (DPM) water depth (the length of pipe from the rig floor to the seafloor) from the total DPM (from the rig floor to the bottom of the hole; see Fig. 1). Note that although the echo-sounding data (from the PDRs) are used to locate the site, they are not used as a basis for any further measurements.

The depth interval assigned to an individual core begins with the depth below the seafloor where the coring operation began, and extends to the depth that the coring operation ended for that core (see Fig. 1). For rotary coring (RCB and XCB), each coring interval is equal to the length of the joint of drill pipe added for that interval (though a shorter core may be attempted in special instances). The drill pipe in use varies from about 9.4 to 9.8 m. The pipe is measured as it is added to the drill string, and the cored interval is recorded as the length of the pipe joint to the nearest 0.1 m. For hydraulic piston coring (APC) operations, the drill string is advanced 9.5 m, the maximum length of the piston stroke.

Coring intervals are not necessarily adjacent, but may be separated by drilled intervals. In soft sediments, the drill string can be "washed ahead" with the core barrel in place, without recovering sediments. This is achieved by pumping water down the pipe at high pressure to wash the sediment out of the way of the bit and up the annulus between the drill pipe and the wall of the hole. If thin, hard, rock layers are present, then it is possible to get "spotty" sampling of these resistant layers within the washed interval, and thus to have a cored interval greater than 9.5 m. In drilling hard rock, a center bit may replace the core barrel should it be necessary to drill without core recovery.

Cores taken from a hole are numbered serially from the top of the hole downward. Core numbers and their associated cored intervals in meters below seafloor usually are unique in a given hole; however, this may not be true if an interval must be cored twice, because of caving of cuttings or other hole problems. Maximum full recovery for a single core is 9.5 m of rock or sediment contained in a plastic liner (6.6 cm internal diameter) plus about 0.2 m (without a plastic liner) in the core catcher (Fig. 2). The core catcher is a device at the bottom of the core barrel that prevents the core from sliding out when the barrel is being retrieved from the hole. For sediments, the core-catcher sample is extruded into a short piece of plastic liner and is treated as a separate section below the last core section. For hard rocks, material recovered in the core catcher is included at the bottom of the last section. In certain situations (e.g., when coring gas-charged sediments that expand while being brought on deck), recovery may exceed the 9.5-m maximum.

A recovered core is divided into 1.5-m sections, numbered serially from the top (Fig. 2). When full recovery is obtained, the sections are numbered from 1 through 7, with the last section possibly being shorter than 1.5 m (rarely, an unusually long core may require more than seven sections). When less than full recovery is obtained, there will be as many sections as needed to accommodate the length of the core recovered; for example, 4 m of core would be divided into two 1.5-m sections and one 1-m section. If cores are fragmented (recovery less than 100%), sections are numbered serially and intervening sections are noted as void, whether or not shipboard scientists think that the fragments were contiguous in-situ. In rare cases, a section

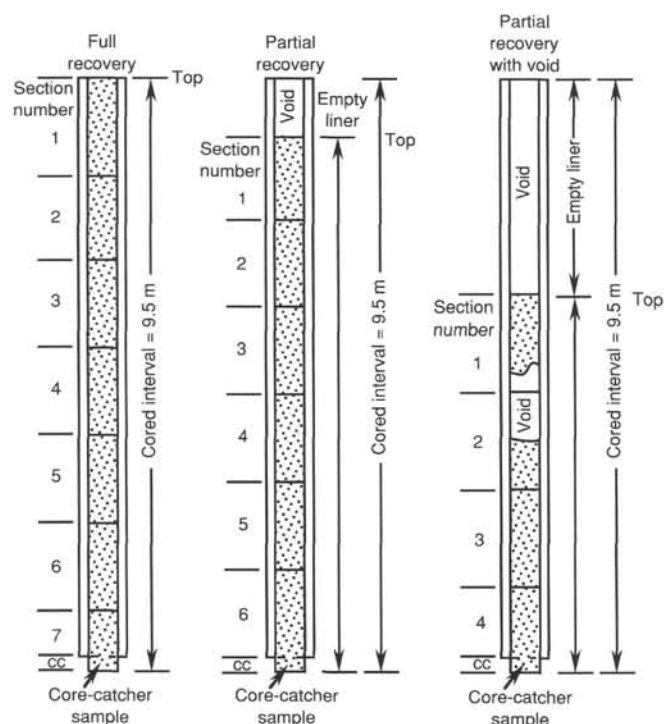


Figure 2. Diagram showing procedure used for cutting and labeling core sections.

less than 1.5 m may be cut to preserve features of interest (e.g., lithological contacts).

By convention, material recovered from the core catcher is placed below the last section when the core is described, and labeled core catcher (CC); in sedimentary cores, it is treated as a separate section. The core catcher is placed at the top of the cored interval in cases where material is recovered only in the core catcher. Information supplied by the drillers or by other sources may allow for more precise interpretation as to the correct position of core catcher material within an incompletely recovered cored interval.

Igneous or metamorphic rock cores are also cut into 1.5-m sections, which are numbered serially; individual pieces of rock are then each assigned a number. Fragments of a single piece are assigned a single number, and individual fragments are identified alphabetically. The core-catcher sample is placed at the bottom of the last section and is treated as part of the last section, rather than separately. Scientists completing visual core descriptions describe each lithologic unit, noting core and section boundaries only as physical reference points.

When, as is usually the case, the recovered core is shorter than the cored interval, the top of the core is equated with the top of the cored interval by convention, to achieve consistency when handling analytical data derived from the cores. Samples removed from the cores are designated by distance measured in centimeters from the top of the section to the top and bottom of each sample removed from that section. In curated hard rock sections (including limestones as well as igneous rocks), sturdy plastic spacers are placed between pieces that did not fit together to protect them from damage in transit and in storage; therefore, the centimeter interval noted for a hard rock sample has no direct relationship to that sample's depth within the cored interval, but is only a physical reference to the location of the sample within the curated core.

A complete identification number for a sample consists of the following information: leg, site, hole, core number, core type, section number, piece number (for igneous and metamorphic rock), and interval in centimeters measured from the top of section. For example, a sample identification of "143-865A-5R-1, 10–12 cm" would be interpreted

as representing a sample removed from the interval between 10 and 12 cm below the top of Section 1, Core 5 (R designates that this core was taken during rotary coring) of Hole 865A during Leg 143.

All ODP core and sample identifiers indicate core type. The following abbreviations are used: R = rotary core barrel (RCB); H = hydraulic piston corer (HPC; also referred to as APC, or advanced hydraulic piston corer); P = pressure core sampler; X = extended core barrel (XCB); B = drill-bit recovery; C = center-bit recovery; I = in-situ water sample; S = sidewall sample; W = wash-core recovery; V = vibrapercussive corer (VPC); and M = miscellaneous material. APC, XCB, RCB drill bits and a diamond core bit (DCB) were used during Leg 143.

## Core Handling

### Sediments

As soon as a core is retrieved on deck, a sample is taken from the core catcher and given to the paleontological laboratory for an initial age assessment. (For the limestones recovered during Leg 143, the recovered cores were often too short to have a core catcher sample. Therefore, the paleontology samples were sometimes taken from Section 1 of those cores. These paleontology samples were used for making thin sections to study microfossils that could not be examined in any other way. After Site 866, the practice of taking paleontology samples from limestones on the catwalk was discontinued because the cores were being split and sampled soon after they were retrieved on deck.) The core is then placed on a long horizontal rack, and gas samples may be taken by piercing the core liner and withdrawing gas into a vacuum tube. Voids within the core are sought as sites for gas sampling. Some of the gas samples are stored for shore-based study, but others are analyzed immediately as part of the shipboard safety and pollution-prevention program. Next, the core is marked into section lengths, each section is labeled, and the core is cut into sections. Interstitial-water (IW) whole-round samples are then taken. In addition, some headspace gas samples are scraped from the ends of cut sections on the catwalk and sealed in glass vials for light hydrocarbon analysis. Each section is then sealed at the top and bottom by gluing on color-coded plastic caps: blue to identify the top of a section and clear for the bottom. A yellow cap is placed on the section ends from which a whole-round sample has been removed, and the sample code (e.g., IW) is written on the yellow cap. The caps are generally attached to the liner by coating the end liner and the inside rim of the cap with acetone, and then the caps are taped to the liners.

The cores then are carried into the laboratory, where the sections are again labeled, using an engraver to make a permanent mark of the complete designation of the section. The length of the core in each section and the core-catcher sample are measured to the nearest centimeter; this information is logged into the shipboard CORELOG database program.

Whole-round sections from APC and XCB cores are normally run through the multisensor track (MST). The MST includes the GRAPE (gamma-ray attenuation porosity evaluator) and *P*-wave logger devices, which measure bulk density, porosity, and sonic velocity, and also includes a meter that determines the volume magnetic susceptibility. Relatively soft sedimentary cores are equilibrated to room temperature (approximately 3 hr) should thermal conductivity measurements be performed on them.

Cores of soft material are split lengthwise into working and archive halves. The softer cores are split with a wire or saw, depending on the degree of induration. In well-lithified sediment cores, the core liner is split and the top half removed so that the whole-round core can be observed before choosing whole-round samples for physical properties (PP) and macrofossil paleontology. Harder cores are then split with a band saw or diamond saw. The wire-cut cores are split from the bottom to top, so investigators should be aware that older material may have been transported up the core on the split face of each section.

The working half of the core is sampled for both shipboard and shore-based laboratory studies. Each extracted sample is logged into the sampling computer database program by its location and the name of the investigator receiving the sample. Records of all removed samples are kept by the curator at the ODP Gulf Coast Repository. The extracted samples are sealed in plastic vials or bags and labeled. Samples are routinely taken for shipboard PP analysis. These samples are subsequently used for calcium carbonate (coulometric analysis) and organic carbon (CNS elemental analyzer), and the data are reported in the site chapters.

The archive half is described visually. Smear slides of soft sediment are made from samples taken from the archive half and are supplemented by thin sections (of both soft sediments and hard rocks) taken from the working half. Smear-slide and thin-section descriptions are entered into the SLIDES database, and the smear slides and thin sections are curated at the ODP Gulf Coast Repository. Most archive sections are run through a cryogenic magnetometer. The archive half is then photographed with both black-and-white and color film, a whole core at a time. Close-up photographs (black-and-white) are taken of particular features for illustrations in the summary of each site, as requested by individual scientists.

Both halves of the core are then placed into labeled plastic tubes, sealed, and transferred to cold-storage space aboard the drilling vessel. Leg 143 cores were transferred from the ship in refrigerated airfreight containers to cold storage at the ODP Gulf Coast Repository, Texas A&M University, College Station, Texas.

### ***Igneous and Metamorphic Rocks***

Igneous and metamorphic rock cores are handled differently from sedimentary cores. Once on deck, the core catcher is placed at the bottom of the core liner, and total core recovery is calculated by shunting the rock pieces together and measuring to the nearest centimeter; this information is logged into the shipboard core-log database program. The core is then cut into 1.5-m-long sections and transferred into the laboratory.

The contents of each section are transferred into 1.5-m-long sections of split core liner, where the bottom of oriented pieces (i.e., pieces that clearly could not have rotated top to bottom about a horizontal axis in the liner) are marked with a red wax pencil. This is to ensure that orientation is not lost during the splitting and labeling processes. Important primary features of the cores are also recorded at this time. The core is then split into archive and working halves. A plastic spacer is used to separate individual pieces and/or reconstructed groups of pieces in the core liner. These spacers may represent a substantial interval of no recovery. Each piece is numbered sequentially from the top of each section, beginning with number 1; reconstructed groups of pieces are assigned the same number, but are lettered consecutively. Pieces are labeled only on external surfaces. If the piece is oriented, an arrow is added to the label pointing to the top of the section. Normally, as pieces are free to turn about a vertical axis during drilling, azimuthal orientation of a core is not possible. However, Leg 143 was the first leg where the sonic core monitor (SCM), the tensor orienting tool, and the scribing core shoe were used together to permit orientation of some hard rock cores.

When splitting the core, every effort is made to ensure that important features are represented in both halves. The working half is sampled for shipboard PP measurement, magnetic studies, X-ray fluorescence (XRF), X-ray diffraction (XRD), and thin-section studies. Nondestructive PP measurements, such as magnetic susceptibility, are performed on the archive half of the core. Where recovery permits, samples are taken from each lithologic unit. Some of these samples are minicores. The archive half was described on the visual core description (VCD) form and is photographed before storage.

The working half of the hard-rock core is then sampled for shipboard laboratory studies. Records of all samples are kept by the curator at ODP.

The archive half is described visually, then photographed with both black-and-white and color film, one core at a time. Both halves of the core are then shrink-wrapped in plastic to prevent rock pieces from vibrating out of sequence during transit, placed into labeled plastic tubes, sealed, and transferred to cold-storage space aboard the drilling vessel. As with the other Leg 143 cores, these are housed at the ODP Gulf Coast Repository.

## **VISUAL CORE DESCRIPTIONS**

### **Sediment Core Description**

#### ***Core Description Forms and the "VCD" Program***

The core description forms (Fig. 3), or "barrel sheets," summarize the data obtained during shipboard analysis of each sediment core. During Leg 143, these were generated using the ODP Macintosh application "VCD" (edition 1.0.1 B8, customized for this leg). The following discussion explains the ODP conventions used for compiling each part of the core description forms, the use of "VCD" to generate these forms, and the exceptions to these procedures adopted by the Leg 143 shipboard party.

Shipboard sedimentologists were responsible for visual core logging, smear-slide analyses, and thin-section descriptions of sedimentary and volcanoclastic material. Core descriptions were initially recorded by hand on a section-by-section basis on standard ODP "Visual Core Description" forms (VCD forms, not to be confused with the "VCD" Macintosh application). Use of these forms is now considered optional by ODP, and during some recent legs, visual description was performed directly at the core-by-core level, using the "VCD" application. During Leg 143, however, we considered that it was desirable to preserve fine-detail observations that are lost at the core-by-core "barrel sheet" level. The "Visual Core Description" forms are available from ODP on request.

Hand-drawn "barrel sheets," used by ODP up through Leg 135, included columns for information about biostratigraphic zonations, geochemistry ( $\text{CaCO}_3$ ,  $\text{C}_{\text{org}}$ , XRF), paleomagnetism, and physical properties (wet-bulk density and porosity). Much of this information is somewhat redundant at the core-by-core level. Core description forms generated directly by the "VCD" Macintosh application comprise a condensed version of the information normally recorded on the section-by-section "Visual Core Description" sheets, supplemented only by a column indicating age. However, the "VCD" application offers an alternative representation of the core description forms as a PICT file, allowing for their manipulation by Macintosh graphics applications. By this means, it is possible to attach columns having additional graphics or text information (e.g., magnetostratigraphy, chemical data, GRAPE data, magnetic susceptibility) as desired.

Customization of the VCD application permitted the addition of sedimentary structures, graphic lithologies, and other features specific to this leg.

#### ***Core Designation***

Cores are designated using leg, site, hole, core number, and core type, as discussed in a preceding section (see "Numbering of Sites, Holes, Cores, and Samples" section, this chapter). The cored interval is specified in terms of meters below sea level (mbsl) and meters below seafloor (mbsf). On the basis of drill-pipe measurements (DPM), reported by the SEDCO coring technician and the ODP operations superintendent, depths are corrected for the height of the rig-floor dual elevator stool above sea level to give true water depth and correct depth in meters below sea level.

#### ***"Graphic Lithology" Column***

The lithology of the recovered material is represented in the core description forms by as many as three symbols in the column titled

SITE 842 HOLE A CORE 999H CORED 0.0 - 0.0 mbsf

Meter	Graphic lith.	Section	Age	Structure and Components	Disturb.	Sample	Color	Description
<div style="text-align: center;">0.5</div> <div style="text-align: center;">1.0</div>		1						
		2						
		3						
		4						
		5						
		6						

Figure 3. Core description form ("barrel sheet") used for sediments and sedimentary rocks.

"Graphic Lithology" (Fig. 4). Where an interval of sediment or sedimentary rock is a homogeneous mixture, the constituent categories are separated by a solid vertical line, with each category represented by its own symbol. Constituents accounting for <10% of the sediment in a given lithology (or others remaining after the representation of the three most abundant lithologies) are not shown in the "Graphic Lithology" column, but are listed in the "Lithologic Description" section of the core description form. In an interval having two or more sediment lithologies with different compositions, such as in thin-bedded and highly variegated sediments, the average relative abundances of the lithologic constituents are represented graphically by dashed lines that vertically divide the interval into appropriate fractions, as described above. The "Graphic Lithology" column shows only the composition of layers or intervals exceeding 20 cm in thickness.

#### "Age" Column

The chronostratigraphic unit, as recognized on the basis of paleontological and paleomagnetic criteria, is shown in the "Age" column in the core description forms. Boundaries between assigned ages are indicated as follows:

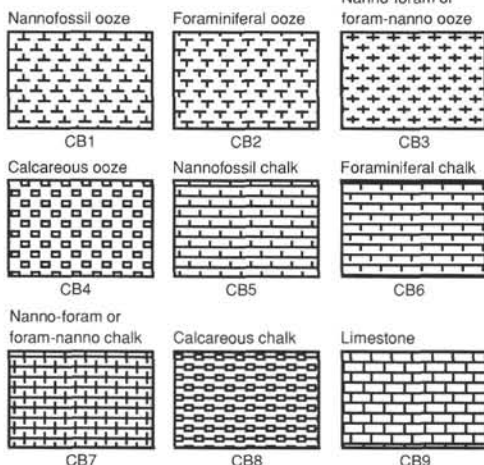
1. Sharp boundary: straight line;
2. Unconformity or hiatus: line with + signs above it; and
3. Uncertain: line with question marks.

#### Sedimentary Structures and Components

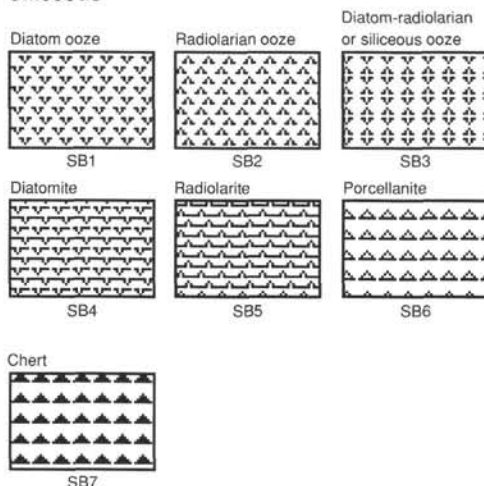
In sediment cores, natural structures and structures created by the coring process can be difficult to distinguish. Natural structures ob-

## PELAGIC SEDIMENTS

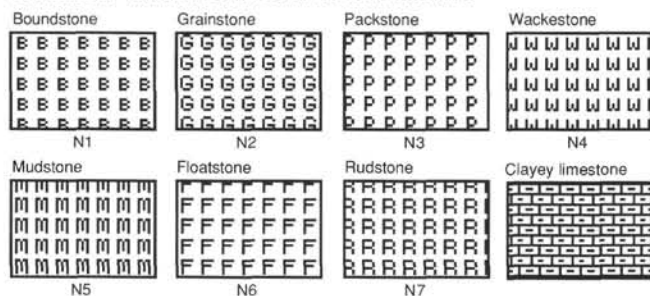
## Calcareous



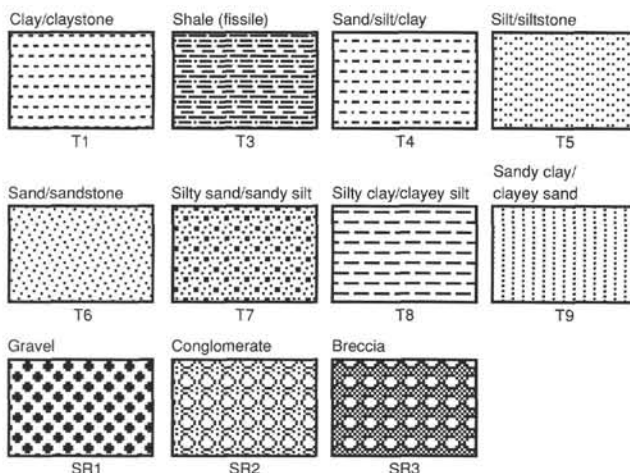
## Siliceous



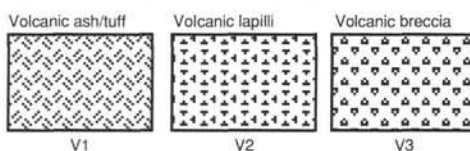
## SHALLOW-WATER CARBONATE SEDIMENTS



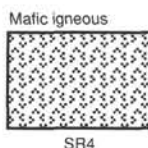
## SILICICLASTIC SEDIMENTS



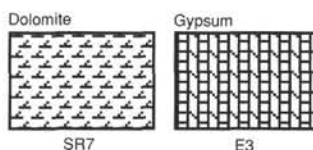
## VOLCANICLASTIC SEDIMENTS



## SPECIAL ROCK TYPES



## CHEMICAL SEDIMENTS



## MIXED SEDIMENTS

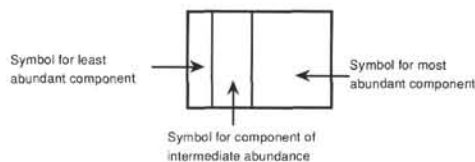


Figure 4. Key to symbols used in the "Graphic Lithology" column of the core description form shown in Figure 3.

served are indicated in the "Structure and Components" column of the core description forms. Sedimentary components, particularly of shallow-water carbonates such as ooids, algae, bryozoans, etc., were also indicated in the "Structure and Components" column by custom symbols created during this leg. The column is divided into three vertical areas for symbols (Fig. 5).

*Sediment Disturbance*

Sediment disturbance resulting from the coring process is illustrated in the "Disturbance" column in the core description forms (using

symbols in Fig. 5). Blank regions indicate the absence of drilling disturbance. The degree of drilling disturbance is described for soft and firm sediments using the following categories:

1. Slightly deformed: bedding contacts are slightly bent.
2. Moderately deformed: bedding contacts are extremely bowed.
3. Highly deformed: bedding is completely disturbed, in some places showing symmetrical diapirlike or flow structures.
4. Soupy: intervals are water-saturated and have lost all aspects of original bedding.

The degree of fracturing in indurated sediments and igneous rocks is described using the following categories:

1. Slightly fractured: core pieces are in place and contain little drilling slurry or breccia;
2. Moderately fragmented: core pieces are in place or partly displaced, but original orientation is preserved or recognizable (drilling slurry may surround fragments);
3. Highly fragmented: pieces are from the interval cored and probably in correct stratigraphic sequence (although they may not represent the entire section), but original orientation is completely lost;
4. Drilling breccia: core pieces have lost their original orientation and stratigraphic position and may be mixed with drilling slurry.

### Color

The hue and chroma attributes of color were determined by comparison with Munsell soil-color charts (Munsell Soil Color Charts, 1971) as soon as possible after the cores were split, because redox-associated color changes may occur when deep-sea sediments are exposed to the atmosphere. Information about core colors is given in the "Color" column in the core description forms.

### Samples

The position of samples taken from each core for shipboard analysis is indicated in the "Samples" column in the core description form, as follows:

- S: Smear slide,
- T: Thin section,
- P: Physical-properties sample,
- M: Micropaleontology sample,
- X: Paleomagnetic sample,
- I: Interstitial-water sample,
- C: Organic-geochemistry sample,
- D: XRD sample,
- F: XRF sample, and
- A: Acetate peels.

### Lithologic Description - Text

The lithologic description that appears in each core description form consists of three parts: (1) a heading that lists all the major sediment lithologies (see "Sedimentology" section, this chapter) observed in the core; (2) a heading for minor lithologies, and (3) a more detailed description of these sediments, including features such as color, composition (determined from the analysis of smear slides), sedimentary structures, or other notable characteristics. Descriptions and locations of thin, interbedded, or minor lithologies that cannot be depicted in the "Graphic Lithology" column are included in the text.

### Smear Slide Summary

A figure summarizing data from smear slides appears in each site chapter, and a table summarizing data from smear slides and thin sections appears at the end of each site chapter. The table includes information about the sample location, whether the sample represents a dominant ("D") or a minor ("M") lithology in the core, and the estimated percentages of sand-, silt-, and clay-size material, together with all identified components. In many cored intervals, the lithology is highly variable on scales of 10 cm to 10 m.

## SEDIMENTARY PETROLOGY

The different core lithologies drilled during Leg 143 were described based upon a modified sediment classification scheme pro-

posed by the Ocean Drilling Program (Mazzullo et al., 1987). For Leg 143 classification, we kept the two basic sediment and rock types described in Mazzullo et al. (1987) as (I) granular and (II) chemical sediments and rocks.

As shown in Table 1, the granular sediments and rocks were subdivided into two lithologic groups: (1) the calcareous lithologies and (2) the siliceous lithologies. The calcareous and siliceous lithologies were then separated into two classes: (A) pelagic and (B) nonpelagic calcareous sediments and rocks, the latter in this case being largely constituted by particles generated in shallow water. Hence pelagic sediments are viewed as essentially biogenic, and the classification of the deep-sea brown (red) clay becomes somewhat problematic. The nonpelagic siliceous class has been subdivided in two subclasses: (a) the siliciclastics and (b) the volcanoclastics.

The graphic symbols utilized are those typically used to represent pelagic sediments. However, to illustrate the range of organisms constituting the shallow-water carbonate lithologies, we have embellished the traditional designs for these facies. In addition we found it useful to adopt the term "clayey limestone", with an appropriate legend, for those limestones that contain substantial amounts of clay minerals and that might, in the field, be appropriately described as "marly."

### Classes of Granular Sediments and Rocks









Five grain types occur in granular sediments and rocks as (1) pelagic calcareous, (2) siliceous particles, (3) nonpelagic calcareous, (4) siliciclastic, and (5) volcanoclastic particles; their definitions are as follows:

1. Pelagic grains are fine-grained skeletal debris produced within the upper part of the water column in open-marine environments by
  - A. Calcareous microfauna, microflora (foraminifers, pteropods, and nannofossils), and associated organisms, and
  - B. Siliceous microfauna, microflora (radiolarians, diatoms), and associated organisms.
2. Nonpelagic grains are coarse- to fine-grained particles deposited in hemipelagic and nearshore environments as
  - A. Calcareous skeletal and nonskeletal grains and fragments (e.g., bioclasts, peloids, micrite). Note that the term micrite is used to define very fine calcareous particles ( $<10\ \mu\text{m}$ ), with no clear identification of origin observed in smear slides. They can be either recrystallized nannofossils or nonpelagic, atoll-derived calcareous mud in pelagic lithologies.
  - B. Siliciclastic grains comprising minerals and rock fragments that were eroded from plutonic, sedimentary, and metamorphic rocks.
  - C. Volcanoclastic grains comprising glass shards, rock fragments, and mineral crystals that were produced by volcanic processes.

Variations in the relative proportions of these five grain types define four major classes of granular sediments and rocks: (1) calcareous and siliceous pelagic, (2) nonpelagic calcareous, (3) siliciclastic, and (4) volcanoclastic sediments and rocks.

Pelagic sediments and rocks contain  $\geq 50\%$  pelagic grains,  $\leq 50\%$  nonpelagic calcareous, siliciclastic, and volcanoclastic grains. Nonpelagic calcareous sediments and rocks include  $\geq 50\%$  nonpelagic calcareous grains,  $\leq 50\%$  pelagic plus nonpelagic siliciclastic and volcanoclastic grains. Siliciclastic sediments and rocks are composed of  $\geq 50\%$  or more siliciclastic grains,  $\leq 50\%$  pelagic plus nonpelagic calcareous and volcanoclastic grains. Volcanoclastic sediments and rocks contain  $\geq 50\%$  volcanoclastic grains,  $\leq 50\%$  pelagic plus nonpelagic calcareous and siliciclastic grains. Volcanoclastics include epiclastic sediments (eroded from volcanic rocks by wind, water, or ice), pyroclastic sediments (products of explosive magma degassing), and hydroclastic sediments (granulation of volcanic glass by steam explosions).

## Drilling disturbance symbols

Soft sediments	
	Slightly disturbed
	Moderately disturbed
	Highly disturbed
	Soupy
Hard sediments	
	Slightly fractured
	Moderately fractured
	Highly fractured
	Drilling breccia

## Sedimentary components and structures
















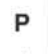


















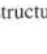
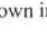
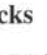

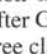
	Red algae		Coated grain
	Green algae		Vugs
	Blue-green algae (Cyanobacteria)		Keystone vugs
	Benthic foraminifers		Bird's-eye vugs
	Planktonic foraminifers		Hardground
	Serpulids		Dolomite
	Rudist bivalves		Glauconite
	Other bivalves		Phosphorite
	Gastropods		Manganese
	Hermatypic corals		Pyrite
	Solitary corals		Chert
	Echinoderms		Lithoclast
	Bryozoan		Bioturbation, minor
	Plant debris		Bioturbation, moderate
	Shell fragments		Bioturbation, strong
	Pellets		Planar laminae
	Peloids		Wavy laminae
	Ooids		Cross-laminae
	Oncoids		Fining-upward sequence
			Desiccation crack

Figure 5. Symbols used for drilling disturbance and sedimentary structures and components in core description forms shown in Figure 3.

## Classification of Granular Sediments and Rocks

Sediment and rock names were defined solely on the basis of composition and texture. Composition becomes more important for description of those deposits more characteristic of open-marine (pelagic) conditions, with texture becoming more significant for the classification of hemipelagic and nearshore (nonpelagic) facies. Data about composition and texture of cored sediments and rocks were primarily determined aboard the ship by (1) unaided visual observation, (2) visual observation using hand lens, and (3) visual estimates in smear slides, thin sections, acetate peels, and coarse fractions with the aid of a microscope. Calcium carbonate content was qualitatively estimated in smear slides and quantitatively estimated by using coulometric analyses (see "Organic Geochemistry" section, this chapter). Other geologic features determined were color and firmness. Colors of the recovered material were determined with Munsell Soil Color charts immediately after the cores were split and while they were still wet. Qualitative evaluations of mineral composition of indurated nonpelagic limestones were obtained by staining of selected samples with alizarin-red S, following the methods outlined in Lewis (1984).

## Firmness

The determination of induration is highly subjective, and the categories used during Leg 143 (after Gealy et al., 1971) are thought to be practical and significant. Three classes of firmness for calcareous sediments and rocks were recognized:

1. Unlithified: soft sediments that have little strength and are readily deformed under the pressure of a fingernail or the broad blade of a spatula. This corresponds to the term *ooze* for pelagic calcareous sediments. In nonpelagic calcareous sediments, the prefix *unlithified* is used (e.g., unlithified packstone).

2. Partly lithified: firm and friable sediments that can be scratched with a fingernail or the edge of a spatula blade. This corresponds to the term *chalk* for pelagic calcareous materials. In nonpelagic calcareous sediment, the prefix *partly lithified* is used (e.g., partly lithified grainstone).

3. Lithified: hard, nonfriable cemented rock, difficult or impossible to scratch with a fingernail or the edge of a spatula. This corresponds to the term *limestone* (lithified ooze) for pelagic calcareous

**Table 1. Outline of the granular sediment classification scheme used during Leg 143.****I. GRANULAR SEDIMENTS AND ROCKS****1. Calcareous lithologies****A. Pelagic sediments and rocks**

Ooze:	Nannofossil ooze	- CB1
	Foraminiferal ooze	- CB2
	Nanno-foram or	
	Foram-nanno ooze	- CB3
	Calcareous ooze	- CB4
Chalk:	Nannofossil chalk	- CB5
	Foraminiferal chalk	- CB6
	Nanno-foram or	
	Foram-nanno chalk	- CB7
	Calcareous chalk	- CB8
Limestone:	Limestone	- CB9

**B. Nonpelagic sediments and rocks - modified for degree of firmness**

(U = unlithified, PL = partially lithified, L = lithified)

	Boundstone	- N1
	Grainstone	- UGR, PLGR, LGR
	Packstone	- UPK, PLPK, LPK
	Wackestone	- UWK, PLWK, LWK
	Mudstone	- N5
	Floatstone	- UFT, PLFT, LFT
	Rudstone	- ULRD, PLRD, LRD

**2. Siliceous lithologies****A. Pelagic sediments and rocks**

	Diatom ooze	- SB1
	Radiolarian ooze	- SB2
	Diatom-radiolarian or	
	Siliceous ooze	- SB3
	Diatomite	- SB4
	Radiolarite	- SB5
	Porcellanite	- SB6
	Chert	- SB7
	Spiculite	SB8

**B. Nonpelagic sediments and rocks****a. Siliciclastic sediments and rocks**

	Clay	- T1
	Shale (fissile)	- T3
	Sand/silt/clay	- T4
	Silt	- T5
	Sand	- T6
	Silty sand - sandy silt	- T7
	Silty clay - clayey silt	- T8
	Sandy clay - clayey sand	- T9
	Gravel	- SR1
	Conglomerate	- SR2
	Breccia	- SR3

**b. Volcaniclastic sediments and rocks**

	Volcanic ash/tuff	- V1
	Volcanic lapilli	- V2
	Volcanic breccia	- V3

**II. CHEMICAL SEDIMENTS AND ROCKS****1. Carbonaceous sediments and rocks**

	Coals and peat	- SR6
	Sapropels	- SR9

**2. Evaporites**

	Halite	- E1
	Anhydrite	- E2
	Gypsum	- E3

**3. Silicates**

	Porcellanite	- SB6
	Chert	- SB7

**4. Carbonates**

	Dolomites	- SR7
--	-----------	-------

material. In nonpelagic calcareous material, the prefix *lithified* is used (e.g., lithified floatstone).

There are only two classes of firmness for *siliceous sediments and rocks*:

1. Soft: sediment core can be split with a wire cutter. Soft terrigenous sediment, pelagic clay, and transitional calcareous sediments are termed sand, silt, or clay.

2. Hard: the core is hard (i.e., consolidated or well indurated) if it must be cut with a hand or diamond saw. For these materials, the suffix “-stone” is added to the soft-sediment name (e.g., sandstone, siltstone, and claystone). Note that this varies from terms used to describe nonpelagic calcareous sediments, for which the suffix “-stone” has no firmness implications.

**X-ray Diffraction Analyses**

A Phillips ADP 3720 X-ray diffractometer was used for the X-ray diffraction (XRD) analyses of mineral phases. CuK $\alpha$  radiation was measured through a Ni filter at 40 kV and 35 mA. The goniometer scanned from 2° to 70° 2 $\theta$  with a step size of 0.01°, and the counting time was 0.5 S/step.

Samples were ground in steel containers in a Spex 8000 mixer mill or with an agate pestle and mortar. This powder was then pressed into the sample holders or mixed with water, placed on glass slides with a pipette, and dried. The glass slides were then mounted with parafilm into sample holders for analysis.

**Principal Names**

We classified granular sediments during Leg 143 by designating a principal name and major and minor modifiers. The principal name of a granular sediment defines its granular-sediment class; the major and minor modifiers describe the texture, composition, fabric, and/or roundness of the grains themselves.

Each granular-sediment class has a unique set of principal names. For pelagic sediments and rocks, the principal name describes the composition and degree of consolidation using the following terms:

1. *Ooze*: unconsolidated calcareous and/or siliceous pelagic sediment;
2. *Chalk*: firm pelagic sediment composed predominantly of calcareous pelagic grains;
3. *Limestone*: hard pelagic sediment composed predominantly of calcareous pelagic grains;
4. *Radiolarite*, *diatomite*, and *spiculite*: firm pelagic sediment composed predominantly of siliceous radiolarians, diatoms, and sponge spicules, respectively;
5. *Porcellanite*: a well-indurated rock with abundant authigenic silica but less hard, lustrous, or brittle than chert (in part, such rocks may represent mixed sedimentary rock);
6. *Chert*: vitreous or lustrous, conchoidally fractured, highly indurated rock composed predominantly of authigenic silica.

The principal name describes the texture and fabric, using the amplification of the original Dunham (1962) classification for nonpelagic calcareous sediments and rocks, according to depositional texture by Embry and Klovan (1971; Fig. 6). The following terms apply:

1. *Mudstone*: mud-supported fabric, with less than 10% grains, grains <2 mm in size;
2. *Wackestone*: mud-supported fabric, with greater than 10% grains, grains <2 mm in size;
3. *Packstone*: grain-supported fabric, with intergranular mud, grains <2 mm in size;
4. *Grainstone*: grain-supported fabric, no mud, grains <2 mm in size;
5. *Floatstone*: matrix-supported fabric, grains >2 mm in size;
6. *Rudstone*: grain-supported fabric, grains >2 mm in size;
7. *Boundstone*: components organically bound during deposition;
8. *Bafflestone*: formed by organisms that act as baffles;
9. *Bindstone*: formed by organisms that encrust and bind; and
10. *Framestone*: formed by organisms that build a rigid framework.

For siliciclastic sediments, texture provides the main criterion for selection of a principal name. The Udden-Wentworth grain-size scale

Allochthonous limestones original components not organically bound during deposition						Autochthonous limestones original components organically bound during deposition		
Less than 10% > 2mm components				Greater than 10% > 2mm components		Boundstone		
						By organisms which act as barriers	By organisms which encrust and bind	By organisms which build a rigid framework
Contains lime mud (< 0.03mm)		No lime mud	Matrix supported	> 2mm component supported				
Mud supported					Grain supported			
Less than 10% grains (> 0.03mm to < 2mm)	Greater than 10% grains							
Mudstone	Wackestone	Packstone			Grainstone	Floatstone	Rudstone	Bafflestone

Figure 6. The Dunham (1962) classification of limestones according to depositional texture, as modified by Embry and Klovan (1971).

(Fig. 7) defines the grain-size ranges and the names of the textural groups (*gravel*, *sand*, *silt*, and *clay*) and subgroups (*fine sand*, *coarse silt*, etc.). When two or more textural groups or subgroups are present, the principal names appear in order of increasing abundance. Eight major textural categories can be defined on the basis of relative proportions of sand, silt, and clay (See Table 1). However, in practice, distinctions between some of the categories are dubious without accurate measurements of weight percentages. This is particularly true for the boundary between silty clay and clayey silt. The suffix “-stone” is affixed to the principal names sand, silt, and clay when the sediment is lithified. The terms “*conglomerate*” and “*breccia*” are the principal names of gravels with well-rounded and angular clasts, respectively.

For volcanoclastic sediments, the principal name is also dictated by the texture. The names and ranges of three textural groups (from Fisher and Schmincke, 1984) are as follows:

1. *Volcanic breccia*: pyroclasts greater than 64 mm in diameter;
2. *Volcanic lapilli*: pyroclasts between 2 and 64 mm in diameter (when lithified, the term “lapillistone” is used); and
3. *Volcanic ash*: pyroclasts less than 2 mm in diameter (when lithified, the term “tuff” is used).

At Site 869, we observed sediments containing obviously pelagic calcareous grains (e.g., foraminifers and coccoliths) mixed with nonpelagic calcareous material (e.g., fine-grained microcrystalline calcite particles and various shallow-water grains). This nonpelagic fine-grained component evidently was produced on the neighboring atoll (Pikinni), transported offshore as suspended load, and subsequently settled through the water column along with the pelagic particles. Following the description of Schlager and James (1978), these mixed sediments presumably represent *periplatform oozes* and *chalks*, but cannot be accurately diagnosed because primary aragonite and high-

magnesian calcite have been diagenetically altered to low-magnesian calcite. Hence, fine calcareous particles observed in addition to nanofossils in smear slides were termed *micrite* and used as a major (25%-40%) or minor (10%-25%) modifier. Sediment and rock with no obvious pelagic calcareous particles, but a large proportion of micrite, would then be classified with the Dunham classification either as a mudstone or a packstone, according to the proportion of grains.

#### Major and Minor Modifiers

To describe the lithology of the granular sediments and rocks in greater detail, the principal name of a granular-sediment class is preceded by major modifiers and followed by minor modifiers. Minor modifiers are preceded by the term “with.” The most common use of major and minor modifiers is to describe the composition and textures of grain types that are present in major (25%-40%) and minor (10%-25%) proportions. In addition, major modifiers can be used to describe grain fabric, grain shape, and sediment color.

The composition of pelagic grains can be described in greater detail with the major and minor modifiers *nannofossil*, *foraminifer(-al)*, *calcareous*, *diatom(-aceous)*, *radiolarian*, *spicule(-ar)*, and *siliceous*. The terms *calcareous* and *siliceous* are used to describe sediments that are composed of calcareous or siliceous pelagic grains of uncertain origin.

The compositional terms for nonpelagic calcareous grains include the following major and minor modifiers as skeletal and nonskeletal grains:

1. *Bioclast* (or *bioclastite*): fragment of skeletal material not diagnosed in detail;
2. *Ooid* (or *oolith*): spherical or elliptical nonskeletal particles smaller than 2 mm in diameter, having a central nucleus surrounded by a rim with concentric or radial fabric;

Millimeters	$\mu\text{m}$	Phi ( $\Phi$ )	Wentworth size class	
4096		-20		
1024		-12	Boulder (-8 to -12 $\Phi$ )	
256		-10		
64		-8	Cobble (-6 to -8 $\Phi$ )	
16		-6		
4		-4	Pebble (-2 to -6 $\Phi$ )	
		-2		
3.36		-1.75		Gravel
2.83		-1.50	Granule	
2.38		-1.25		
2.00		-1.00		
1.68		-0.75		
1.41		-0.50	Very coarse sand	
1.19		-0.25		
1.00		0.00		
0.84		0.25		
0.71		0.50	Coarse sand	
0.59		0.75		
1/2	500	1.00		Sand
0.42	420	1.25		
0.35	350	1.50	Medium sand	
0.30	300	1.75		
1/4	250	2.00		
0.210	210	2.25		
0.177	177	2.50	Fine sand	
0.149	149	2.75		
1/8	125	3.00		
0.105	105	3.25		
0.088	88	3.50	Very fine sand	
0.074	74	3.75		
1/16	63	4.00		
0.0530	53	4.25		
0.0440	44	4.50	Coarse silt	
0.0370	37	4.75		
1/32	31	5		
0.0156	15.6	6	Medium silt	
1/128	7.8	7	Fine silt	
1/256	3.9	8	Very fine silt	
0.0020	2.0	9		Mud
0.00098	0.98	10		
0.00049	0.49	11		
0.00024	0.24	12	Clay	
0.00012	0.12	13		
0.00006	0.06	14		

Figure 7. Udden-Wentworth grain-size classification of terrigenous sediments (from Wentworth, 1922).

3. *Pisolite*: spherical or ellipsoidal non-skeletal particle, commonly greater than 2 mm in diameter, with or without a central nucleus, but displaying multiple concentric layers of carbonate;

4. *Oncoid* (or *oncolite*): spherical or spheroidal stromatolite, displaying multiple concentric layers of carbonate produced by the trapping and binding action of cyanobacteria;

5. *Pellet* (-al): fecal particles from deposit-feeding organisms;

6. *Peloid* (*pel*): micritized carbonate particle of unknown origin;

7. *Intraclast*: reworked carbonate-sediment/rock fragment or rip-up clast consisting of the same lithology as the host sediment;

8. *Lithoclast*: reworked carbonate-rock fragment consisting of a lithology different from the host sediment;

9. *Rudistid*: containing abundant rudistid fragments;

10. *Echinodermal*: containing abundant echinoderm fragments;

11. *Algal*: containing abundant algal debris;

12. *Coral-rich*: containing abundant coral debris;

13. *Gastropod-rich*: containing abundant gastropod debris;

14. *Molluscan*: containing abundant unspecified molluscan debris.

The textural designations for siliciclastic grains use standard major and minor modifiers, such as *gravel*(-ly), *sand*(-y), *silt*(-y), and *clay*(-ey) (Shepard, 1954). The character of siliciclastic grains can be described further by mineralogy (using modifiers such as "quartz," "feldspar," "glaucinite," "mica," "kaolinite," "zeolitic," "lithic," "calcareous," "gypsiferous," or "sapropelic." In addition, the provenance of rock fragments (particularly in gravels, conglomerates, and breccias) can be described by modifiers such as volcanic, sed-lithic, meta-lithic, gneissic, and plutonic. The fabric of a sediment can be described as well using major modifiers such as grain-supported, matrix-supported, and imbricated. Generally, fabric terms are useful only when describing gravels, conglomerates, and breccias.

The composition of volcanoclastic grains is described by the major and minor modifiers *lithic* (rock fragments), *vitric* (glass and pumice), and *crystal* (mineral crystals). Modifiers can also be used to describe the compositions of the lithic grains and crystals (e.g., *feldspathic* or *basaltic*).

### Classes of Chemical Sediments and Rocks

Chemical sediments are composed of minerals that formed by inorganic processes, such as precipitation from solution or colloidal suspension, deposition of insoluble precipitates, or recrystallization. Chemical sediments generally have a crystalline (i.e., nongranular) texture. There are five classes of chemical sediments: (1) *carbonaceous* sediments and rocks, (2) *evaporites*, (3) *silicates*, (4) *carbonates*, and (5) *metalliferous* sediments and rocks.

*Carbonaceous* sediments and rocks contain >50% organic matter (plant and algal remains) that has been altered from its original form by carbonization, bituminization, or putrefaction. Examples of carbonaceous sediments include peat, coal, and sapropel (jellylike ooze or sludge of algal remains). The *evaporites* are classified according to their mineralogy using terms such as halite, gypsum, and anhydrite. They may be modified by terms that describe their structure or fabric, such as massive, nodular, and nodular-mosaic. *Silicates* and *carbonates* are defined as crystalline sedimentary rocks that are nongranular and nonbiogenic in appearance. They are classified according to their mineralogy, using principal names such as chert (microcrystalline quartz), calcite, and dolomite. They should also be modified with terms that describe their crystalline (as opposed to granular) nature, such as crystalline, microcrystalline, massive, and amorphous. *Metalliferous* sediments and rocks are nongranular nonbiogenic sedimentary rocks that contain metal-bearing minerals, such as pyrite, goethite, manganese oxyhydroxides, chamosite/berthierine, and glauconite. They are classified according to their mineralogy.

## BIOSTRATIGRAPHY

### Time Scales

The chronostratigraphy used for the Cenozoic follows Berggren et al. (1985a, 1985b). For the Mesozoic, the chronostratigraphic nomenclature and geochronology of Kent and Gradstein (1985) was utilized. The latter time scale has been modified in one place. Recently available radiometric dates of normally magnetized crust from the Ontong Java Plateau (Mahoney et al., in press; Tarduno et al., 1991a, 1991b) lie close to 124 Ma. This basement is overlain by lower Aptian sediments indicating that the age of 119 Ma for the Barremian/Aptian boundary in the Kent and Gradstein (1985) time scale is too young. In addition, the Barremian/Aptian stage boundary lies slightly below polarity zone M0 (e.g., Tarduno et al., 1989). In the middle Cretaceous quiet zone, the ages of zonal boundaries were taken directly from the Kent and Gradstein (1985) time scale for Albian and younger stages. Although we note problems in applying

the Kent and Gradstein (1985) time scale, it is beyond the scope of this study to recalculate a new time scale.

## Biostratigraphy

### Calcareous Nannofossils

Cenozoic calcareous nannofossil zonation of Martini (1971) was applied during Leg 143. This worked well for the Paleocene, Oligocene and younger intervals but most Eocene markers were very rare or absent. The zonation scheme of Bukry (1973) was also inapplicable in this interval. We therefore relied on secondary markers compiled by Perch-Nielsen (1985).

In the Mesozoic, no developed zonation has demonstrated worldwide applicability (Mutterlose, in press), and this is evident in the central Pacific. In the Upper Cretaceous (Turonian-Maastrichtian) the zonations of Sissingh (1977) and Roth (1978) were not applicable in numerous intervals either because of the absence of markers or because of the order of events observed. Therefore we have used particular zones from each zonation scheme. Middle Cretaceous (Albian-Cenomanian) zonations proved to be more successful and were compiled from Thierstein (1971, 1973) and Roth (1978), with modifications from Bralower (1988) and Bralower et al. (in press) that significantly increase potential biostratigraphic resolution.

### Planktonic Foraminifers

Age assignments were based mainly on core-catcher samples. Additional samples were studied when zone boundaries or unconformities were observed. For the Neogene, we followed the zonation of Blow (1969), as amended by Kennett and Srinivasan (1983). The Pliocene/Pleistocene boundary, between Zones N21 and N22, was taken at the first occurrence of *Globorotalia truncatulinoides*. The Miocene/Pliocene boundary, between Zones N18 and N19, is based on the first occurrence of *Sphaeroidinella dehiscentis*, and the Oligocene/Miocene boundary is equated with the first diversification of the genus *Globigerinoides* within the range of *Paragloborotalia kugleri*. This event is close to the first occurrence of *Globoquadrina dehiscentis*. For the Paleogene, the tropical zonation of Blow (1969) was applied to the upper Eocene-Oligocene section, and Berggren et al.'s (1985a) zonation was used for the Paleocene-middle Eocene. In the Cretaceous, the zonations of Caron (1985) and Sliter (1989) were combined and used in both nonindurated and indurated sediments.

### Cretaceous Benthic Foraminifers

Benthic foraminiferal biostratigraphy for the Lower Cretaceous is based on distribution charts for the Adriatic Area and Northern Margin of the Tethys prepared by the Working Group on Benthic Foraminifers of the IGCP Project No. 262 "Tethyan Cretaceous Correlation." Completed charts will be published as part of the final report.

Our paleobathymetric interpretations for Cretaceous benthic foraminifers follow those of Sliter (1986).

### Rudists

Rudists were visible at random orientations on the sides of core pieces before the cores were split. Care was taken to ensure that whole rudists and large fragments were not cut accidentally during splitting and these pieces were kept as whole rounds.

The requieniid rudists recovered from Site 865 did not in general need further treatment as the external morphology (which is revealed when the rock splits naturally into drilling biscuits) is most useful in their determination.

Caprinid rudists found at Sites 866, 867, and 868 were selected in a similar manner and examined first on the core surfaces of whole rounds. In identification of these rudists, orientated sections are often required to reveal the shape of internal canals. Most were sufficiently

robust so that they could be sliced with the rock saw and the surfaces polished. More fragile material in a friable matrix could only be cut after impregnation with epoxy which took place on shore.

No standard reference work is entirely suitable for the identification of these faunas; the Treatise (Deschaseaux et al., 1969) is not recommended. Coogan (1977), which has a compilation of descriptions of the Early Cretaceous Gulf Coast faunas, may be useful as a general guide (although the identification of *Planocaprina* and *Præcaprina*, which are crucial to this work, includes some probable errors; see Skelton, 1982). To best understand the taxonomic status of these faunas comparisons must be made on a case-by-case basis with descriptions from the literature (however inadequate these may be) and references given in the appropriate section. All rudist ranges reported in the literature are at best approximate and most are based on the ranges of co-occurring benthic foraminifers.

## Methods and Procedures

### Calcareous Nannofossils

Nannofossil samples for biostratigraphic examination were prepared by making simple smear slides from raw sediment samples. Smear slides were preferred over gravity settling because of a possible tendency for the latter process to exclude smaller specimens. The technique of Monechi and Thierstein (1985) was utilized to prepare slides from lithified samples. Slides were observed in the light microscope on board the ship.

Estimates of the relative abundance of calcareous nannofossils in pelagic/hemipelagic sediments, where they usually constitute a sizable fraction of the sediment, were determined following these guidelines:

- VA (Very Abundant) > 20 specimens/field of view,
- A (Abundant) > 10 specimens/field of view,
- C (Common) 1–10 specimens/field of view,
- F (Few) 1 specimen/2–10 fields of view,
- R (Rare) 1 specimen/11–100 fields of view,
- VR (Very Rare) 1 specimen/>100 fields of view.

All estimates were made at a magnification of 1250 $\times$ .

In shallow-water carbonates, in which nannofossils composed a smaller fraction of the total sediment, a different scale for estimating relative abundance was utilized:

- A (Abundant) > 100 specimens observed,
- C (Common) 1–10 specimens observed,
- F (Few) 3–10 specimens observed,
- R (Rare) 1–2 specimens observed.

These estimates were made after two traverses (200 fields of view) of a slide at a magnification of 1250 $\times$ . In all samples, regardless of age, an estimate was made of the total nannofossil abundance in the following fashion. Nannofossils were listed as

- A (abundant), if they account for more than 10% of all particles,
- C (common), if they account for 1–10%,
- F (few), if they account for 0.1–1%,
- R (rare), if they account for less than 0.1%.

An estimate of the average preservational state of all nannofossil taxa was given for each slide. An average is necessary because certain species are more susceptible to overgrowth and/or dissolution than others. Letters representing preservation states were designated as follows:

- E (Excellent) - No evidence of any overgrowth/dissolution on any specimens,
- G (Good) - Only slight overgrowth/dissolution of most specimens,

M (Moderate) -Most specimens display modest degrees of overgrowth/dissolution; species identification not impaired.

P (Poor) -Most specimens display significant amounts of overgrowth/dissolution; species identification sometimes impaired.

VP (Very Poor) - All specimens display profound overgrowth/dissolution; species identification impossible.

In addition, a description of the degree of etching and overgrowth was given in particularly important intervals, following the guidelines of Roth and Thierstein (1972). The symbol "E" indicates the degree of etching, with "E-1," "E-2," and "E-3" indicating slight, moderate, and severe etching, respectively. Similarly "O-1," "O-2," and "O-3" indicate slight, moderate, and severe overgrowth, respectively.

### Foraminifers

Most samples were disaggregated in a hot detergent solution, with hydrogen peroxide and Calgon added to the clayey samples. Samples were washed over a 43- $\mu$ m sieve and dried under a heat lamp. The relative abundance of species in an assemblage was based on a visual estimate of the >43- $\mu$ m residue (no actual counts were made). The following categories were used to indicate abundance:

A = Abundant(>30%),  
C = Common(15%–30%),  
F = Few (3%–15%),  
R = Rare (<3%).

Preservational characteristics were divided into three categories:

G = Good (>90% of the specimens unbroken),  
M = Moderate (30%–90% of the specimens show dissolved or broken chambers),  
P = Poor (sample dominated by fragments and most specimens broken and severely corroded).

### Palynomorphs

Calcareous sediments were disaggregated with HCl. Samples were then washed and centrifuged to remove acid. Organic residue was then placed on a cover slip, spread out with a toothpick, and dried. Cover slips were mounted on slides using Norland optical adhesive. Generally, only core-catcher samples were analyzed, although where lithologies within the cores were palynologically important (such as organic-rich layers), a core sample was also processed.

## PALEOMAGNETISM

Measurements for Leg 143 differed with lithology and coring method. For APC cores, pass-through measurements were performed at a 5-cm spacing. The natural remanent magnetization (NRM) and magnetization after demagnetization at 15 mT were routinely recorded. For material obtained using the rotary core system, the primary shipboard paleomagnetic scanning technique was the measurement of standard minicores (2.54 cm diameter). On the rare occasions when the rotary core system resulted in the recovery of long continuous core pieces, archive (halves of) cores were also measured, and the results were used to guide further shipboard sampling. Alternating field (AF) demagnetization was limited to those archive sections where the NRM measurements indicated that the remanence was stable and the intensity was above the lower practical limit of operation of the shipboard cryogenic magnetometer (about 0.01 mAm<sup>-1</sup>). Measurements of the standard paleomagnetic minicores consisted of magnetic susceptibility (prior to demagnetization), NRM, and progressive AF demagnetization.

Magnetic susceptibility of whole-core sections was measured as part of the physical properties package (see "Physical Properties"

section, this chapter). Measurements were collected at 3-to 10-cm intervals in sections having good recovery.

### Sediments

The magnetization of many of the sediments was very weak, frequently less than 0.1 mAm<sup>-1</sup>. Measurement of discrete specimens from many intervals was therefore reserved for land-based studies, where more sensitive magnetometers would be available. Demagnetization of more strongly magnetized sediments, however, permitted directions of the characteristic remanent magnetization (ChRM) to be isolated by the removal of secondary components, predominantly viscous remanent magnetizations (VRMs) and magnetizations acquired during drilling. The magnetic polarity was determined in some sedimentary intervals, allowing for the construction of tentative magnetostratigraphies. We consider such polarity assignments to be at best "working models," testable by further shore-based studies.

### Basalts

ChRM directions were derived from the measurement of discrete basalt samples and pass-through measurements of long continuous basalt pieces. These inclination data were averaged into discrete, sequential "virtual inclination" groups and combined to provide estimates of paleolatitude. As in the case of the sedimentary data, we consider the presented paleolatitude estimates to be preliminary and a guide to further work.

### Time Scales

Reference was made to the time scales of Berggren et al. (1985a, 1985b) and Kent and Gradstein (1985) (Table 2). There are several reasons why these works were chosen in preference to the more recent time scale presented by Harland et al. (1990). Although some radiometric data do support the older age of 124 Ma used by Harland et al. (1990) for reversed polarity Chron M0 (CM0), the placement of this chron with respect to stage is incorrect in the Harland et al. (1990) scale. Previous magnetostratigraphic and biostratigraphic data from DSDP Site 463 indicate that CM0 falls entirely within the Aptian (Tarduno et al., 1989), and not on the Aptian/Barremian boundary as suggested by Harland et al. (1990) (see Tarduno et al., 1991a, 1991b, for further discussion). Although even more recent work has suggested major modifications of the classical assignment of foraminiferal zones to stage (see "Biostratigraphy" section, this chapter), no such evidence exists for similar shifts in nannofossil datums. The placement of CM0 entirely in the lower Aptian, as used by Kent and Gradstein (1985), is the most consistent assignment, given the available data. As the identification of CM0 is crucial to the Albian-Barremian sequences studied during Leg 143, Kent and Gradstein's (1985) scale provides the best reference relating magnetostratigraphy, geologic stage, and micropaleontological zonations.

### Magnetic Remanence

During Leg 143 magnetic remanence was measured with the shipboard 2-G Enterprises (Model 760R) three-axis, pass-through cryogenic superconducting rock magnetometer, which is integrated with an on-line AF demagnetizer (Model 2G600) capable of alternating fields up to 20 mT. ODP policy limits demagnetization of archive sections to 15 mT. The cryogenic magnetometer was operated in two modes. For archive sections, standard pass-through measurements were performed. For discrete samples, measurements were taken at each of seven positions that corresponded to the placement of minicores in the sample holder. The SQUID sensors measure magnetization over an interval approximately 15 cm long. Each axis has a slightly different response curve. For archive sections, the widths of the sensor regions imply that as much as 150 cm<sup>3</sup> of core contributes

Table 2. Geomagnetic polarity time scale for the Cenozoic and Late Cretaceous<sup>a</sup> and the Early Cretaceous and Late Jurassic.<sup>b</sup>

Normal polarity interval (Ma)	Anomaly	Normal polarity interval (Ma)	Anomaly	Reversed anomaly	Normal polarity interval (Ma)	Normal anomaly	Reversed anomaly	Normal polarity interval (Ma)	Normal anomaly
0–0.73	1	23.55–23.79	6C		84.00–118.00	Cret. Quiet Zone	PM26	158.01–158.21	
0.91–0.98		24.04–24.21	6C	M0	118.70–121.81		PM27	158.37–158.66	
1.66–1.88	2	25.50–25.60	7	M1	122.25–123.03	M2	PM28	158.87–159.80	
2.02–2.04		25.67–25.97	7	M3	125.36–126.46	M4	PM29	160.33–(169.00)	Jur. Quiet Zone
2.12–2.14		26.38–26.56	7A	M5	127.05–127.21				
2.47–2.92	2A	26.86–26.93	8	M6	127.34–127.52				
2.99–3.08	2A	27.01–27.74	8	M7	127.97–128.33				
3.18–3.40	2A	28.15–28.74	9	M8	128.60–128.91				
3.88–3.97	3	28.80–29.21	9	M9	129.43–129.82				
4.10–4.24	3	29.73–30.03	10	M10	130.19–130.57				
4.40–4.47	3	30.09–30.33	10		130.63–131.00				
4.57–4.77	3	31.23–31.58	11		131.02–131.36				
5.35–5.53	3A	31.64–32.06	11	M10N	131.65–132.53				
5.68–5.89	3A	32.46–32.90	12	M11	133.03–133.08				
6.37–6.50		35.29–35.47	13	M11	133.50–134.01				
6.70–6.78	4	35.54–35.87	13		134.42–134.75				
6.85–7.28	4	37.24–37.46	15	M12	135.56–135.66				
7.35–7.41	4	37.48–37.68	15		135.88–136.24				
7.90–8.21	4A	38.10–38.34	16		136.37–136.64				
8.41–8.50	4A	38.50–38.79	16	M13	137.10–137.39				
8.71–8.80		38.83–39.24	16	M14	138.30–139.01				
8.92–10.42	5	39.53–40.43	17	M15	139.58–141.20				
0.54–10.59		40.50–40.70	17	M16	141.85–142.27				
11.03–11.09		40.77–41.11	17	M17	143.76–144.33				
11.55–11.73	5A	41.29–41.73	18	M18	144.75–144.88				
11.86–12.12	5A	41.80–42.23	18		144.96–145.98				
12.46–12.49		42.30–42.73	18	M19	146.44–146.75				
12.58–12.62		43.60–44.06	19		146.81–147.47				
12.83–13.01		44.66–46.17	20	M20	148.33–149.42				
13.20–13.46		48.75–50.34	21	M21	149.89–151.46				
13.69–14.08		51.95–52.62	22		151.51–151.56				
14.20–14.66		53.88–54.03	23		151.61–151.69				
14.87–14.96	5B	54.09–54.70	23	M22	152.53–152.66				
15.13–15.27	5B	55.14–55.37	24		152.84–153.21				
16.22–16.52	5C	55.66–56.14	24		153.49–153.52				
16.56–16.73	5C	58.64–59.24	25	M23	154.15–154.48				
16.80–16.98	5C	60.21–60.75	26		154.85–154.88				
17.57–17.90	5D	63.03–63.54	27	M24	155.08–155.21				
18.12–18.14	5D	64.29–65.12	28		155.48–155.84				
18.56–19.09	5E	65.50–66.17	29		156.00–156.29				
19.35–20.45	6	66.74–68.42	30	M25	156.55–156.70				
20.88–21.16	6A	68.52–69.40	31		156.78–156.88				
21.38–21.71	6A	71.37–71.65	32		156.96–157.10				
21.90–22.06		71.91–73.55	32		157.20–157.30				
22.25–22.35		73.96–74.01			157.38–157.46				
22.57–22.97	6B	74.30–80.17	33		157.53–157.61				
23.27–23.44	6C	84.00–118.00	34		157.66–157.85				

<sup>a</sup> After Berggren et al. (1985a, 1985b).<sup>b</sup> After Kent and Gradstein (1985).

to the sensor signals. The large volume of core material within the sensor region permits an accurate determination of remanence for relatively weakly magnetized samples, despite the relatively high background noise related to the motion of the ship. For archive sections, declinations and inclinations are best determined by deconvolution of the  $x$ ,  $y$ ,  $z$  data. No deconvolution program was available for Leg 143, however, so declination and inclination were calculated directly from the  $x$ ,  $y$ ,  $z$  data, while intensity was calculated by dividing the magnetic moment by the volume of the sample within the sensors (i.e., the length within the sensor region by the cross-sectional area of the core). AF demagnetization of discrete samples was performed with a Schonstedt Model GSD-1 AC demagnetizer. Demagnetizations were routinely repeated in opposite directions to test for the acquisition of a spurious anhysteretic remanent magnetization.

### Magnetic Susceptibility

Magnetic susceptibility of whole-round core sections was measured with a Bartington Instruments magnetic susceptibility meter

(Model M.S.1) with an 80 mm sensing loop. Measurements were typically made with a 3 to 5 cm spacing. Because the measured susceptibility depends on sample volume, only relatively full sections of core were routinely measured. Leg 143 sediments were weakly magnetic, so the meter was operated on its most sensitive setting (0.1 scale) which gives a sensitivity of  $10^{-7}$  cgs. Susceptibility values were measured in cgs units rather than SI, because shipboard software is designed to handle the former. Nevertheless, the conversion to SI units is simple,  $K_{\text{cgs}} = 4\pi K_{\text{SI}}$ , where  $K$  is volume susceptibility. An additional correction is necessary for both sets of units to correct for the ratio of core diameter to coil diameter; this is done by multiplying the measured susceptibility by 0.63.

## INORGANIC GEOCHEMISTRY

### Interstitial-Water Chemistry

The shipboard inorganic geochemistry program focused on the retrieval of interstitial waters by means of hydraulic-press actuated extrusion of samples obtained from 5- to 10-cm-long, whole- or

half-round core sections. The exteriors of these core samples were carefully scraped with spatulas to remove contaminated surfaces before being placed into stainless steel presses and then into a hydraulic squeezer, as described by Manheim and Sayles (1974). Under pressure, the interstitial waters flowed through 0.45- $\mu\text{m}$  Gelman acrodisc disposable filters into plastic syringes and then subsequently subdivided for both shipboard work as well as for future work in shore laboratories. Care was taken that the end caps were not sealed with acetone prior to taking the inorganic geochemistry whole-round samples. Additional precautions were taken to minimize the effects of core contamination by drill water through the removal of any suspicious material from the outside of the whole-core sample and along cracks and fissures.

Interstitial-water samples were routinely analyzed for salinity, pH, alkalinity, chlorinity, calcium, magnesium, sulfate, silica, phosphate, ammonium, sodium, potassium, strontium, rubidium, and lithium.

The routine measurements of the interstitial waters were performed as follows: salinities with a hand-held Goldberg optical refractometer; pH and alkalinity by Gran titration using a Brinkmann pH electrode and a Metrohm autotitrator;  $\text{Cl}^-$ ,  $\text{Ca}^{+2}$  and  $\text{Mg}^{+2}$  concentrations by titration;  $\text{SO}_4$  with a DIONEX 2120i chromatograph;  $\text{Si}^{+4}$ ,  $\text{PO}_4$  and  $\text{NH}_4$  with colorimetric techniques using a Milton Roy Spectronic 1001 spectrophotometer.

The standard seawater of the International Association of Physical Sciences Organizations (IAPSO) was used to calibrate most of these techniques. Chemical data are reported in molar units.

Shipboard analyses performed are listed in Table 3. All these techniques were performed as described by Gieskes et al. (1991).

### Atomic Absorption/Emission Analysis

The atomic absorption (AA) procedures used during ODP cruises have been described in detail by Gieskes et al. (1991) and in the Leg 133 "Explanatory Notes" chapter (Davies, McKenzie, Palmer-Julson, et al., 1991). We used flame spectrophotometric techniques with a Varian SpectrAA-20 AA unit to quantify concentrations of  $\text{Na}^+$ ,  $\text{K}^+$ ,  $\text{Li}^+$ ,  $\text{Sr}^{+2}$ , and  $\text{Rb}^+$ . Standards for analyzing potassium and sodium were prepared by diluting IAPSO (399.43 ppm K) with distilled (nanopure) water. The 1/200 diluted aliquots, which remain from  $\text{SO}_4$  analysis, were used for preparing final dilution (1/10) and were analyzed by flame emission using an air-acetylene flame (Varian AA at 766.5-nm wavelength) with 3.5% CsCl solution as an ionization suppressant.

Lithium values were determined for 1/30 diluted aliquots by emission using an air-acetylene flame; standards were prepared from a  $\text{LiCl}_2$  (50 mM) solution.

Strontium was measured in the absorption mode at 460.7 nm using an air/acetylene flame. Standards were prepared using a stock 1000-ppm  $\text{Sr}^{+2}$  solution. Standards of 1, 2, 5, 10, and 15 ppm were prepared. Samples were diluted using a 50,000-ppm La solution to a dilution of 1:20. This method was found to provide reproducible results.

Rubidium was determined directly from undiluted interstitial water samples by emission using an air-acetylene flame. Standards were prepared from a 100-ppm Rb reference solution. Standards for all flame spectrophotometric techniques were matched in matrix composition to the samples.

## ORGANIC GEOCHEMISTRY

The shipboard organic geochemistry program for Leg 143 included (1) measurement of inorganic carbon concentration; (2) elemental analysis of total nitrogen, carbon, and sulfur; (3) determination of free hydrocarbons, petroleum potential, and maturity of organic matter; (4) analyses of volatile hydrocarbons; and (5) pyrolysis-gas chromatography from selected samples. The detailed procedures have been described by Emeis and Kvenvolden (1986).

**Table 3. Analytical methods for inorganic geochemistry used during Leg 143.**

Analysis	Technique	Reference
Salinity	Goldberg refractometer	Gieskes et al. (1991)
Alkalinity	Gran titration	Gieskes et al. (1991)
pH	TRIS-BIS buffers	Bates and Calais (1981)
		Bates and Culberson (1977)
Calcium	EGTA titration	Tsunogai et al. (1968)
Magnesium	EDTA titration	Gieskes et al. (1991)
Strontium	Absorption spectrometry	
Rubidium	Emission spectrometry	
Lithium	Emission spectrometry	
Sodium	Emission spectrometry	
Potassium	Emission spectrometry	
Chlorinity	Mohr titration	
Ammonia	Colorimetry	Solorzano (1969)
		Gieskes (1973)
Phosphate	Colorimetry	Strickland and Parsons (1968),
		Gieskes (1973)
Silica	Colorimetry	Gieskes (1973)

### Inorganic Carbon

Inorganic carbon was determined using a coulometric 5011 carbon dioxide coulometer equipped with a System 140 carbonate-carbon analyzer. A known mass ranging from 15 to 70 mg of freeze-dried, ground, and weighed sediment was reacted in a 2N HCl solution. The liberated  $\text{CO}_2$  was titrated in a monoethanolamine solution with a coulometric indicator, while the change in the light transmittance was monitored with a photo-detection cell. The percentage of carbonate was calculated from the inorganic carbon (IC) content, assuming that all carbonate occurs as calcite, as follows:

$$\text{CaCO}_3 = \text{IC} \cdot 8.33$$

No corrections were done for siderite or dolomite.

### Elemental Analysis

Total nitrogen, carbon, and sulfur contents were determined using an N/C/S analyzer, Model NA1500 from Carlo Erba Instruments. Mixtures of vanadium pentoxide and crushed samples were combusted in an oxygen atmosphere at 1000°C, converting organic and inorganic carbon to  $\text{CO}_2$ , sulfur to  $\text{SO}_2$ , and nitrogen to  $\text{NO}_2$ . The  $\text{NO}_2$  was subsequently reduced to  $\text{N}_2$  using copper. The gases were then separated by gas chromatography and measured with a thermal conductivity detector. Total organic carbon (TOC) was calculated by difference between total carbon (TC) and inorganic carbon:

$$\text{TOC} = \text{TC} - \text{IC}$$

### Organic Matter Characterization and Maturation

The characters of the organic carbon in the sediments was determined with a Geofina hydrocarbon meter (GHM). The GHM is a modified Varian 3400 gas chromatograph with three flame ionization detectors (FID), two capillary columns, and a sample injector. This system generated three types of information from the organic material: (1) free hydrocarbons, termed  $\text{S}_1$ , released at 300°C; (2) the amount of hydrocarbons (termed  $\text{S}_2$ ) that were produced (mainly as result of the cracking of kerogen) during heating from 300° to 540°C; and (3) the temperature of maximum hydrocarbon production during pyrolysis. This temperature is equivalent to the  $T_{\text{max}}$  in Rock-Eval pyrolysis (Espitalié et al., 1977, 1985, 1986). From the  $\text{S}_2$  values provided by GHM and the total organic carbon concentrations furnished by elemental analysis, the hydrogen and production indexes (HI and PI, respectively) were calculated. The hydrogen index repre-

sented the ratio of pyrolyzable organic matter or "hydrocarbons" ( $S_2$ ) to total organic carbon (mg HC/g TOC). The production index (PI) was defined as the ratio  $S_1/(S_1+S_2)$ . The petroleum potential was calculated as the sum of  $S_1 + S_2$ .

### Volatile Hydrocarbons

For safety considerations, concentration of methane ( $C_1$ ) and ethane ( $C_2$ ) gases were monitored at 30-m intervals or whenever gas pockets were encountered. Gases were extracted using a headspace-sampling technique for bulk sediments (Kvenvolden and McDonald, 1986), or a vial for sampling gas pockets directly through the core liner. The headspace analyses were performed by placing 5-cm<sup>3</sup> samples in glass containers (sealed with a septum and metal crimp) and heating them to 70°C. All gas samples were analyzed with a Carle AGC series 100/Model 211. Samples that were determined to contain notable quantities of low-molecular-weight hydrocarbons were also analyzed with a Hewlett Packard 5890 gas chromatograph.

### Pyrolysis-gas Chromatography

The Geofina hydrocarbon meter (GHM) also yields a rapid evaluation of the origin of organic matter. This determination is accomplished by gas chromatography (GC) analysis of the thermal extracts and pyrolysis products of rock samples. The type of organic matter is recognized qualitatively by GC fingerprint traces.

## IGNEOUS PETROLOGY

### Visual Core Descriptions

Visual core description (VCD) forms for "igneous and metamorphic rocks" were used in the documentation of the igneous rock cores. The left column is a graphic representation of pieces comprising the archive half of the core. A horizontal line across the entire width of the column denotes a plastic spacer. Vertically oriented pieces are indicated on the form by an upward-pointing arrow to the right of the piece. Shipboard samples and studies are indicated in the column headed "Shipboard studies," using the following notation: XRD = X-ray diffraction analysis; XRF = X-ray fluorescence analysis; TSB = petrographic thin section; PP = physical properties analysis; and PMAG = paleomagnetic analysis.

To ensure consistent and complete descriptions, the visual core descriptions were entered into the computerized database HARVI. The database is divided into separate data sets for fine-grained and coarse-grained rocks. Fine-grained rocks are either aphyric or phyric with a microcrystalline to glassy matrix, whereas coarse-grained rocks are holocrystalline with groundmass minerals that are visible with the aid of a 10× hand lens. Each record is checked by the database program for consistency and completeness and is subsequently printed in a format that can be pasted directly onto the barrel sheet for subsequent curatorial handling.

When describing sequences of rocks, the core was subdivided into lithologic units on the basis of changes in rock mineralogical composition and modal abundance, texture, and rock clast type. For each lithologic unit and section, the following information was recorded in the database system:

1. The leg, site, hole, core number, core type, and section number.
2. The unit number (consecutive downhole), position in the section, number of pieces of the same lithologic type, the rock name, and the identification of the describer.
3. The Munsell color of the rock when dry and the presence and character of any deformation.
4. The mineral phases visible with a hand lens and their distribution within the unit, together with the following information for each

phase: (A) abundance (vol%); (B) size range in millimeters; (C) shape; (D) degree of alteration; and (E) further comments.

5. The groundmass texture: glassy, fine grained (<1 mm), medium grained (1–5 mm), or coarse grained (>5 mm). Grain-size changes within units were also noted.

6. The presence and characteristics of secondary minerals and alteration products.

7. The abundance, distribution, size, shape, and infilling material of vesicles (including the proportion of vesicles that are filled by alteration minerals).

8. Whether the unit consists of massive flows, thin or sheet flows, pillow lavas, sills, dikes, hyaloclastites, or is brecciated and contains any layering or banding.

9. The relative amount of rock alteration: fresh (<2%); slightly altered (2%–10%); moderately altered (10%–40%); highly altered (40%–80%); very highly altered (80%–95%); and completely altered (95%–100%). The type, form, and distribution of alteration was also noted.

10. The presence of veins and fractures, including their abundance, width, mineral filling, orientation, and wall rock reaction. The relationship of the alteration and vein mineral filling to veins and fractures was also noted.

11. Other comments, including notes on the continuity of the unit within the core and on the interrelationship of units.

Basalt and diabase are termed aphyric (<1%), sparsely phyric (1%–2%), moderately phyric (2%–10%), or highly phyric (>10%), depending upon the proportion of phenocrysts visible with the hand lens or binocular microscope. Basalts are further classified by phenocryst type (e.g., a moderately plagioclase-olivine phyric basalt contains 2%–10% phenocrysts, mostly plagioclase, with subordinate olivine). More specific rock names were assigned whenever thin sections or chemical analyses were available.

Igneous visual core descriptions are given in the section called "Cores" following the site chapters, and descriptions of each rock unit are available from the computerized database at the ODP repositories.

### Thin-section Descriptions

Thin sections of igneous rocks were examined to complement and refine the hand-specimen observations. The percentages and textural descriptions of individual phases were reported in the computerized database HRTIN. The same terminology was used for both thin-section and megascopic descriptions. Thin-section descriptions are included in a separate section in the back of the book and are also available from the ODP computerized database.

### X-ray Fluorescence Analysis

Prior to analysis, samples were crushed in a Spex 8510 shatterbox using a tungsten carbide barrel. At least 20 cm<sup>3</sup> of material was ground to ensure a representative sample. The tungsten carbide barrel introduces considerable W contamination and minor Ta, Co, and Nb contamination, rendering the powder unsuitable for instrumental neutron activation analysis (INAA).

A completely automated wavelength-dispersive ARL8420 XRF (3 kW) system equipped with an Rh target X-ray tube was used to determine the abundances of major oxides and trace elements of whole-rock samples. Analyses of the major oxides were conducted on lithium borate glass disks doped with lanthanum as a "heavy absorber" (Norris and Hutton, 1969). The disks were prepared from 500 mg of rock powder, ignited for 3 to 4 hr at about 1025°C, and mixed with 6.000 g of pre-weighed (on shore) dry flux consisting of 80% lithium tetraborate and 20%  $La_2O_3$ . This mixture was then melted in air at 1150°C in a Pt-Au crucible for about 10 min and poured into a Pt-Au

mold using a Claiss fluxer. The 12:1 flux-to-sample ratio and the use of the lanthanum absorber made matrix effects insignificant over the normal range of igneous rock compositions. Hence, the relationship between X-ray intensity and concentration becomes linear and can be described by

$$C_i = (I_i \cdot m_i) - b_i$$

where  $C_i$  = concentration of element  $i$  (wt%);  $I_i$  = net peak X-ray intensity of element  $i$ ;  $m_i$  = slope of calibration curve for element  $i$  (wt%/cps); and  $b_i$  = apparent background concentration for element  $i$  (wt%).

The slope  $m_i$  was calculated from a calibration curve derived from the measurement of well-analyzed reference rocks (BEN, BR, DRN [from Geostandards, France]; BHVO-1, AGV-1 [from the U.S. Geol. Surv.]; JGB-1, JP-1 [from the Geol. Surv. of Japan]; AII-92-29-1 [from Woods Hole Oceanographic Institution/Massachusetts Institute of Technology]; and K1919 [from Lamont-Doherty Geological Observatory]). The analyses of these standards derived from the calibration curves used are given in Table 4. The background  $b_i$  was determined by regression analysis from the calibration curves.

Systematic errors resulting from short- or long-term fluctuations in X-ray tube intensity and instrument temperature were corrected by normalizing the measured intensities of the samples to those of an internal standard that was run together with a set of six unknown samples. Two glass disks were prepared for each sample. Accurate weighing was difficult on board the moving *JOIDES Resolution*, and was performed with particular care as weighing errors could be a major source of imprecision in the final analysis. Five weight measurements, with weights within 0.5 mg (+0.1%) considered acceptable, were taken for each sample, and the average was used. Loss on ignition (LOI) was determined by drying the sample at 110°C for 8 hr, and then by weighing before and after ignition at 1025°C in air.

Trace elements were determined with pressed-powder pellets prepared by pressing (with 8 MPa of pressure) a mixture of 5.0 g of dry rock powder (dried at 110°C for >2 hr) and 30 drops of polyvinyl alcohol binder into an aluminum cap. A modified Compton scattering technique (based on the intensity of the Rh Compton peak) was used for matrix absorption corrections (Reynolds, 1967).

Replicate analyses of rock standards show that the major element data are precise within 0.5% to 2.5%, and are considered accurate to ~1% for Si, Ti, Fe, Ca, and K, and between 3% and 5% for Al, Mn, Na, and P. The trace element data are considered accurate to within 2% and 3% or 1 ppm (whichever is greater) for Rb, Sr, Y, and Zr, and between 5% and 10% or 1 ppm for most of the others. The accuracy for Ba and Ce is considerably less, and they are primarily for purposes of internal comparison. Precision is within 3% for Ni, Cr, and V at concentrations of >100 ppm, but 10% to 25% at concentrations of <100 ppm. Analytical conditions for the XRF analyses are given in Table 5.

## PHYSICAL PROPERTIES

Shipboard measurements of physical properties provide the basis for geotechnical stratigraphic studies and allow for the calibration of the lithologic record with geophysical site-survey data and downhole logging results. Cores were generally sampled with sufficient density to encompass the range of lithologic units recovered from each hole. Where necessary, because of closer spaced changes in lithology and/or physical properties, additional measurements were obtained. The properties determined include compressional wave velocity, bulk density, grain density, porosity, water content, and thermal conductivity. In all discrete measurements used for determining physical properties, an effort was made to analyze only visually undisturbed sediment and rock. Boyce (1976) described in detail the techniques employed when determining index properties and compressional wave velocity. The two techniques used for shipboard determination of thermal conductivity are those of Von Herzen and Maxwell (1959) and

**Table 4. Analyses of standards derived from the calibrations used for whole-rock geochemical analyses of igneous rocks.**

Run	BHVO P	BHVO Q	BHVO R	BHVO T
Major trace precision standard				
Na <sub>2</sub> O	2.95	2.95	3.01	2.89
MgO	7.10	7.12	7.05	7.08
MnO	0.17	0.17	0.17	0.17
TiO <sub>2</sub>	2.75	2.75	2.74	2.75
K <sub>2</sub> O	0.58	0.59	0.59	0.58
SiO <sub>2</sub>	49.80	50.00	49.94	50.02
CaO	11.40	11.39	11.44	11.41
Fe <sub>2</sub> O <sub>3</sub>	12.20	12.22	12.23	12.19
Al <sub>2</sub> O <sub>3</sub>	13.60	13.64	13.61	13.62
P <sub>2</sub> O <sub>5</sub>	0.28	0.28	0.28	0.28
Total	100.83	101.10	101.06	100.99
Trace precision standard				
Run	BHVO N	BHVO O	BHVO S	
Nb	19	18	18	
Zr	173	172	172	
Y	25	26	26	
Sr	396	395	395	
Rb	9	9	9	
Zn	108	106	106	
Cu	134	136	136	
Ni	123	120	120	
Cr	288	293	293	
V	318	305	305	
TiO <sub>2</sub>	2.70	2.70	2.70	
Ce	30	37	37	
Ba	133	129	129	

Vacquier (1985). Because of a failure of the vane shear apparatus, no vane shear measurements were performed during Leg 143 operations. For similar reasons, no measurements of electric resistivity and formation factor were done during this leg. Bulk density, porosity, compressional wave velocity, and magnetic susceptibility were measured simultaneously by employing the multisensor track (MST). The MST integrates the measurements of several physical properties in whole-round core sections during a single run. The MST incorporates the gamma-ray porosity evaluator (GRAPE),  $P$ -wave logger (PWL), and magnetic susceptibility devices during scans of the whole-round core sections. Individual unsplit core sections were placed horizontally on the MST, which moves the section through the three sets of sensors. Three different methods were used to measure sonic velocity, largely depending on the coherence and competence of the material, which varied from soft unconsolidated to semi-indurated to well-lithified. A summary of the methods employed during Leg 143, in the sequence as the cores were processed in the shipboard laboratory, follows.

### Gamma-ray Attenuation Porosity Evaluator (GRAPE)

The GRAPE technique measures bulk density and porosity in whole APC and XCB cores where the core liner is both undeformed and full of sediment across its entire diameter. The method is based on the attenuation, by Compton scattering, of a collimated beam of gamma rays passing through a known volume of sediment and has been used for measuring sediment density since DSDP Leg 2 (Boyce, 1976). Measurements were performed over two second windows, equivalent to a sample interval of 2.5 cm, while the core was moved with constant speed past the gamma-ray source and sensor. During Leg 143, the GRAPE was calibrated at least once every 24 hr by running an aluminum standard. The GRAPE data were most reliable

Table 5. Leg 143 X-ray diffraction analytical conditions.

Element	Line	Crystal	Detector	Collimator	Peak angle (deg)	Background offset (deg)	Total count time (s)	
							Peak	Background
SiO <sub>2</sub>	K $\alpha$	PET(002)	FPC	Coarse	109.04	0	40	0
TiO <sub>2</sub>	K $\alpha$	LiF(200)	FPC	Fine	86.17	0	40	0
Al <sub>2</sub> O <sub>3</sub>	K $\alpha$	PET(002)	FPC	Coarse	144.47	0	100	0
<sup>54</sup> Fe <sub>2</sub> O <sub>3</sub>	K $\alpha$	LiF(200)	FPC	Fine	57.56	0	40	0
MnO	K $\alpha$	LiF(200)	KrSC	Fine	63.00	0	40	0
MgO	K $\alpha$	TLAP	FPC	Coarse	44.77	$\pm 0.80$	200	400
CaO	K $\alpha$	LiF(200)	FPC	Coarse	113.14	0	40	0
Na <sub>2</sub> O	K $\alpha$	TLAP	FPC	Coarse	54.61	1.20	200	200
K <sub>2</sub> O	K $\alpha$	LiF(200)	FPC	Coarse	136.64	0	100	0
P <sub>2</sub> O <sub>5</sub>	K $\alpha$	Ge(111)	FPC	Coarse	140.98	0	100	0
Rh	K-C	LiF(200)	Scint	Fine	18.63	0	60	0
Nb	K $\alpha$	LiF(200)	Scint	Fine	21.43	$\pm 0.35$	200	200
Zr	K $\alpha$	LiF(200)	Scint	Fine	22.57	$\pm 0.35$	100	100
Y	K $\alpha$	LiF(200)	Scint	Fine	23.82	$\pm 0.40$	100	100
Sr	K $\alpha$	LiF(200)	Scint	Fine	25.17	$\pm 0.41$	100	100
Rb	K $\alpha$	LiF(200)	Scint	Fine	26.63	$\pm 0.60$	100	100
Zn	K $\alpha$	LiF(200)	Scint	Coarse	41.79	$\pm 0.40$	100	100
Cu	K $\alpha$	LiF(200)	Scint	Coarse	45.02	$\pm 0.40$	100	100
Ni	K $\alpha$	LiF(200)	Scint	Coarse	48.71	$\pm 0.60$	100	100
Cr	K $\alpha$	LiF(200)	FPC	Fine	69.39	$\pm 0.50$	100	100
Fe	K $\alpha$	LiF(220)	FPC	Fine	85.75	$-0.40+0.70$	40	40
V	K $\alpha$	LiF(220)	FPC	Fine	123.24	$-0.50$	100	60
TiO <sub>2</sub>	K $\alpha$	LiF(200)	FPC	Fine	86.17	$\pm 0.50$	40	40
Ce	L $\beta$	LiF(220)	FPC	Coarse	128.37	$\pm 1.50$	100	100
Ba	L $\beta$	LiF(220)	FPC	Coarse	128.95	$\pm 1.50$	100	100

<sup>a</sup> Total Fe as Fe<sub>2</sub>O<sub>3</sub>.

FPC = flow proportional counter using P10 gas; KrSC = sealed krypton gas counter; Scint = NaI scintillation counter; Elements analyzed under vacuum using goniometer 1 at generator settings of 60 kV and 50 mA.

in APC cores. In the lithified platform carbonates and underlying volcanics, the GRAPE was turned off.

### Compressional Wave Velocity Logger

The compressional wave velocity logger, or PWL, operated simultaneously with the GRAPE and magnetic susceptibility meter in the MST, has been designed to measure accurately the traveltime of an ultrasonic compressional pulse travelling through a sediment-filled plastic core liner. Acoustic spring-mounted transducers are positioned on either side of the APC and XCB core sections and, thus, parallel to the sediment bedding plane. The acoustic source produces a 500-kHz pulse at a repetition rate of 1000 Hz. The sampling interval used was 2.5 cm. Displacement transducers (mounted behind the ultrasonic transducers) monitor variations in liner diameter. Coupling of the transducers with the cores was achieved by applying distilled water to the core liner. The data were edited on the basis of signal strength; all values for which strength was below 30 were dropped.

The PWL was calibrated with a distilled-water standard at least once for each drill site. The receiver detects the acoustic signal to an accuracy of 50 ns, corresponding to an instrument resolution of 1.5 m/s for sediment obtained using APC and XCB techniques. Absolute accuracy of the technique was estimated at 5 m/s due to variations in thickness of the core liner. Generally, only the APC cores were measured. Once the lithified carbonate platform sediments were penetrated, the PWL was turned off.

### Compressional Wave Velocity

Discrete measurements of sonic velocity in lithified carbonate sediments and volcanics were performed using a Hamilton-Frame velocimeter. *P*-wave velocities were measured in softer sediments (unconsolidated to semiconsolidated pelagic ooze) using a Dalhousie University/Bedford Institute of Oceanography digital sound velocimeter (DSV). Velocity calculation is based on the accurate meas-

urement of the delay time of an impulsive acoustic signal travelling between a pair of piezoelectric transducers inserted in the split sediment cores. The transducers used emit a 2- $\mu$ s square wave at about 250 and 750 kHz. A dedicated microcomputer controls all functions of the velocimeter. The transmitted and received signals are digitized by a Nicolet 320 digital oscilloscope and then transferred to a microcomputer for processing. The DSV software selects the first arrival and then calculates the sediment velocity. The full waveform is stored for calculating attenuation later. Two transducers, separated by approximately 7 cm, were used to measure the vertical (along the core-axis) *P*-wave velocity. These transducers are firmly fixed at one end on a steel plate so that their separation does not change during velocity determinations. Periodically, the separation was precisely evaluated by running a calibration procedure in distilled water. Generally, the results of the velocity measurements in the unlithified pelagic ooze were very near the *P*-wave velocity of seawater. It has been suggested that APC coring liquifies unstable sediments and therefore biases the retrieved data. When coring disturbance seemed less likely, measurements were performed in the middle of every section. Where the sediment showed disturbance (liquefaction), no measurements were taken.

Compressional wave velocity in lithified carbonates and volcanics was measured on discrete samples that were sufficiently competent to provide adequate signal strength. Velocities were calculated from the determination of the traveltime of a 500-kHz compressional wave through a measured thickness of a sample, using a Hamilton-Frame velocimeter and Tektronix DC 5010 counter/timer system. Rock samples were trimmed with a special double-bladed diamond core saw. Zero traveltimes for the velocity transducers were estimated by linear regression of the traveltime vs. distance for a series of aluminum and lucite standards. The DSV oscilloscope was used to calculate velocities. Sampling density largely depended on rate of recovery and therefore was irregular. Where necessary, because of lithologic variation, multiple samples were analyzed. *P*-wave velocity was measured in both longitudinal and transverse directions in cubes (1-in. sides) as well as, when recovery and core quality allowed, in minicores cut from

adjacent samples (1-in. diameter). This approach then provided a measure of the acoustic anisotropy within the sediment. The index of percent of anisotropy was determined by the following relationship:

$$\text{Anisotropy} = 2(V_{pt} - V_{pl})(V_{pt} + V_{pl})^{-1},$$

where  $V_{pt}$  is the transverse compressional wave velocity and  $V_{pl}$  the longitudinal velocity (Carlson and Christensen, 1977). Distilled water was used to improve the acoustic contact between the sample and the transducers. Velocities were not recorded when insufficient or extremely variable signals were obtained.

### Thermal Conductivity

Whole-round cores were allowed to equilibrate to room temperature for 3 to 4 hr before thermal conductivity was measured. The thermal conductivity techniques used were those described by Von Herzen and Maxwell (1959) and Vacquier (1985). All thermal conductivity data have been reported in units of watts per meter degrees Centigrade ( $W/[m \cdot ^\circ C]$ ). Thermal conductivity was calculated from an increase in temperature of a needle measured over a 6-min period of heating. Sampled temperatures from a heating time interval of 60 to 240 s were fitted to a curve using a least-squares approximation as follows:

$$T(t) = F \cdot (q/4Qk) \cdot \ln(t) + A + Bt,$$

where

$k$  = thermal conductivity,

$T$  = temperature,

$t$  = time since heater on,

$q$  = heat input per unit length per unit time,

$A$  and  $B$  = constant of a linear temperature drift, and

$F$  = correction factor determined from calibration tests performed on standards before the measurement program.

Reliable measurements require that the temperature drift in the sample at the time of measurement be less than  $4 \cdot 10^{-2}^\circ C/\text{min}$ .

Needle probes that connected to a Thermcon-85 unit were inserted into the sediment through holes drilled into the core liner, and thermal drift was monitored. Probes were rotated, and one was inserted into a reference material during each run to monitor the probe behavior. Once the temperature had stabilized, the probes were heated and the coefficient of thermal conductivity was calculated as a function of the change in resistance in the probe about every 20 s over a 6-min interval. When the sediment became too stiff to allow for easy insertion of the probe, holes were drilled into the core material before insertion of the probes. An attempt was made to insert the probes at locations along each core section that appeared to be the least disturbed. However, an annulus of disturbed sediment and drill fluid often was present along the inside of the liner and prevented visual identification of the more intact segments in the core.

### Magnetic Susceptibility

Magnetic susceptibility was measured in all sections at 3-cm intervals, using the 0.1 range on the Bartington meter with an 8-cm diameter loop. Close sampling was conducted to provide another measure for between-hole correlation (see "Paleomagnetism" section, this chapter).

### Index Properties

Index properties (bulk density, grain density, water content, porosity, dry density) were calculated from measurements of wet and dry weights and wet and dry volumes. Samples of approximately 10

to  $20 \text{ cm}^3$  were taken for determining index properties. In addition, whole-core determination of bulk density was measured in the pelagic ooze using the GRAPE on the MST.

Sample mass was determined aboard the ship to a precision of 0.03 g using a Scitech electronic balance. The sample mass was counterbalanced by a known mass, such that only mass differentials of less than 0.5 g were measured. The balance was interfaced with a PRO-350 computer, which compensated for the motion of the ship by taking the average of 100 sample weighings. Dry sample weight was determined using the same procedure after oven drying at  $110^\circ C$  for at least 24 hr. Volumes were determined using a Penta-pycnometer, a helium-displacement pycnometer. This pycnometer measures volumes to a precision of  $+0.02 \text{ cm}^3$ . A reference volume was run with each group of samples during the first test series. Preliminary results suggest that the pycnometer is fairly stable for a given cell inset, or sleeve. However, changing sleeves or insets offset the standard calibration by  $0.1 \text{ cm}^3$ .

### Water Content

The determination of water content followed the methods of the American Society for Testing and Materials (ASTM) designation (D) 2216 (ASTM, 1989). As outlined in ASTM D2216, corrections are required for salt when measuring marine samples. The index properties of samples of the unlithified sediment were corrected for salt. No salt correction was done for samples of lithified sediment and basalt because shipboard measuring of total saturated mass (and thus, indirectly, water content) is inaccurate. In the case of Leg 143 sediments, all pore-water salinities were within 1 ppt of 35. The recommended equation for the water content calculation, which is the ratio of the pore-fluid mass to the dry sediment mass (% dry wt), is as follows:

$$Wc(\% \text{ dry wt}) = (Mt - Md)/(Md - rMt),$$

where

$Mt$  = total mass (saturated),

$Md$  = dry mass, and

$r$  = salinity.

### Bulk Density

Bulk density ( $\bar{\rho}$ ) is the density of the total sample, including the pore fluid, or  $\bar{\rho} = Mt/Vt$ , where  $Vt$  is the total sample volume. The mass ( $Mt$ ) was measured using the electronic balance, and total volume was measured using the helium pycnometer. In high-porosity sediments (pelagic ooze), density was calculated directly using  $\bar{\rho} = Mt/Vt$ .

### Porosity

The porosity was calculated using the following equation:

$$\phi = (Wc \cdot \bar{\rho})/[(1 + Wc) \cdot \bar{\rho}_w],$$

where

$\bar{\rho}$  is the directly measured bulk density,

$\bar{\rho}_w$  is the density of the pore fluid, and

$Wc$  is the water content reported as a decimal ratio of %dry wt.

### Grain Density

The grain density was calculated from the dry mass (Scitech balance) and dry volume (pycnometer) measurements. Both mass and volume were corrected for salt as follows:

$$\partial_{\text{grain}} = (Md - s)/(Vd - [s/\partial_{\text{salt}}]),$$

where

$Vd$  = dry mass,

$s$  = salt content, and

$\partial_{\text{salt}}$  = density of salt (2.257 g/cm<sup>3</sup>).

### Dry Density

Dry density is the ratio of the dry mass ( $Md$ ) to the total volume. This value is typically used for calculating mass accumulation. The dry density was calculated using the corrected water content and porosity for each measurement.

Many index property samples were previously measured for compressional wave velocity and carbonate content, and this enabled us to correlate directly between velocity and index properties to check for possible trends and data consistency.

## DOWNHOLE MEASUREMENTS

### Logging Tool Strings

Downhole logs can be used directly to determine physical and chemical properties of formations adjacent to the borehole. Interpretation of these continuous, in-situ measurements can yield stratigraphic, lithologic, geophysical, and mineralogic characterizations of the site. After coring is completed at a hole, a tool string (a combination of several sensors) is lowered down the hole on a seven-conductor cable, and each of the sensors in the tool string continuously monitors some property of the adjacent borehole. Although the depths of investigation are sensor-dependent, data are typically recorded at 15-cm intervals. Three Schlumberger tool strings were used during Leg 143: the geophysical (quad-combo), geochemical, and combinations. The Lamont-Doherty Geological Observatory (Lamont) temperature tool was attached to the base of the first- and last-run tool strings to obtain heat-flow information. The slim-hole digital borehole televiewer was used at Site 866, and the Japanese downhole magnetometer was used at Sites 865, 866, and 869.

The geophysical tool string used during Leg 143 consisted of the long-spaced sonic (LSS), natural spectral gamma-ray (NGT), high-temperature lithodensity (HLD), compensated neutron porosity (CNT-G), mechanical caliper (MCD), and the phasor induction (DIT) tools. The

geophysical tool string measures compressional wave velocity and provides indicators of the two variables that most often control velocity: porosity, as indicated by density, porosity, or resistivity; and clay content, as indicated by the NGT. The sonic velocity data, when combined with information about density, are used to calculate an impedance log and to generate a synthetic seismogram for the logged section. The NGT is run in each tool string to provide a basis for interlog correlations.

The geochemical combination used during Leg 143 consisted of the NGT, aluminum clay tool (ACT), compensated neutron porosity (CNT-G) and induced gamma-ray spectrometry (GST) tools. This tool combination measures the relative concentrations of silicon, calcium, aluminum, iron, sulfur, hydrogen, chlorine, potassium, thorium, and uranium.

The FMS tool string includes not only the FMS, but also a general-purpose inclinometer tool (GPIT) that spatially orients the FMS resistivity map of the borehole wall. This tool string also contains NGT to allow for depth correlation of FMS data with other logs.

### Logging Tools

A brief description of logging tools run during Leg 143 is given in the following section. A detailed description of logging tool principles and applications is provided in Schlumberger (1972), Serra (1984), and Timur and Toksöz (1985).

### Electrical Resistivity

The DIT provides measurements of spontaneous potential (SP) and three different measurements of electrical resistivity, each one having a different depth of investigation. Two induction devices (deep [ILD] and medium [ILM] resistivity) send high-frequency alternating currents through transmitter coils, creating magnetic fields that induce secondary (Foucault) currents in the formation (Fig. 8A). These ground-loop currents produce new inductive signals, proportional to the conductivity of the formation, which are recorded by the receiving coils. Measured conductivities then are converted to resistivity. A third device (spherically focused resistivity (SFLU), Fig. 8B) measures the current necessary to maintain a constant voltage decrease across a fixed interval. Vertical resolution is about 150 cm for the medium device, 200 cm for the deep resistivity device, and about 76 cm for the focused-resistivity device.

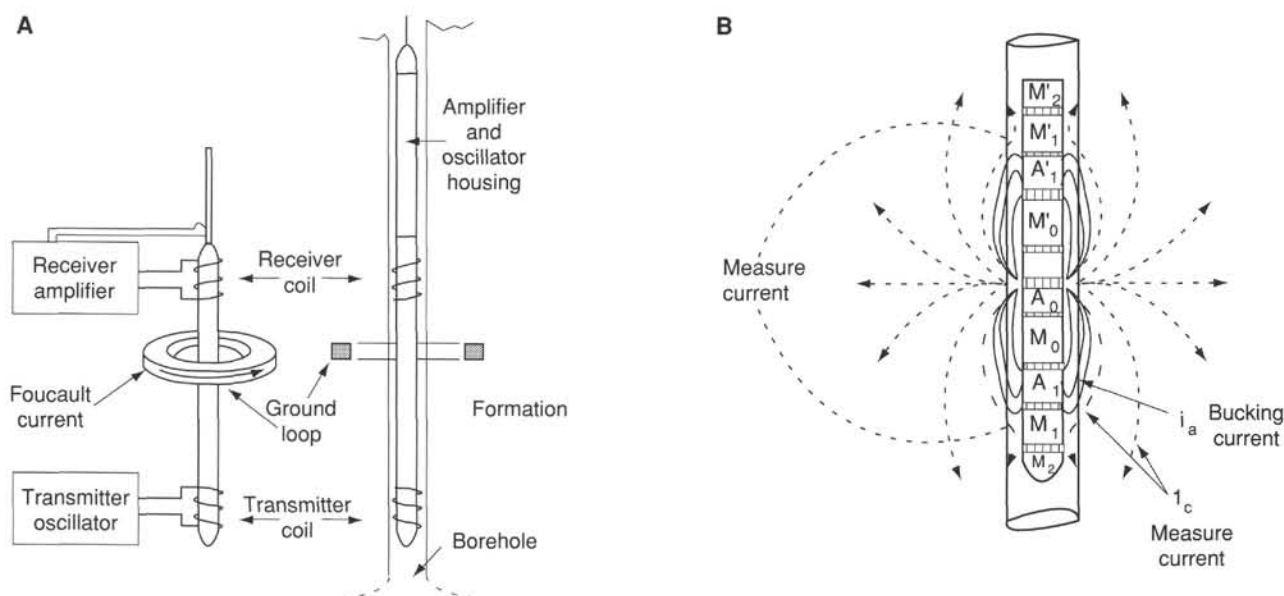


Figure 8. Sketch of Schlumberger resistivity devices. A. DIT. B. SFLU.

Water content and salinity are by far the most important factors controlling the electrical resistivity of rocks. To a first-order approximation, resistivity is proportional to the inverse square root of porosity (Archie, 1942). Other factors influencing resistivity include the concentration of hydrous and metallic minerals, vesicularity, and geometry of interconnected pore space.

### Lamont Temperature Tool

The Lamont temperature tool (LTL) is a self-contained tool that can be attached to any Schlumberger tool string. Data from two thermistors and a pressure transducer are collected at a pre-determined sample rate, between 0.5 and 5.0, and stored in a Tattletale computer within the tool. Following the logging run, data are dumped from the Tattletale to a shipboard computer for analysis. A fast-response, lower-accuracy thermistor can detect sudden, very small temperature excursions caused by fluid flow from the formation. A slow-response, higher-accuracy thermistor can be used to estimate heat flow, provided the history of drilling-fluid circulation in the hole and at least two temperature logs are available (Jaeger, 1961). Data are recorded as a function of time; conversion to depth can be based on the pressure transducer or, preferably, on simultaneous recording by Schlumberger of both depth and time.

### Sonic Velocity Measurements

The LSS tool uses two acoustic transmitters and two receivers to measure the time required for sound waves to travel over source-receiver distances of 2.4, 3.0, and 3.6 m (Fig. 9). These raw data are reported as time required for a sound wave to travel through 0.31 m of formation; these traveltimes are then converted to sonic velocities. First arrivals for the individual source-receiver paths are used to

calculate the velocities of the different waves traveling in the formation (compressional, shear, etc.). Only compressional wave velocity is determined during data acquisition, but waveforms are recorded for post-cruise determination of shear-wave velocities and possibly for improved compressional wave velocities. The vertical resolution of the tool is 60 cm. Compressional wave velocity is dominantly controlled by porosity and degree of lithification; both decreases in porosity and increases in lithification cause the velocity to increase.

### Natural Gamma-ray Tool

The NGT measures the natural radioactivity of the formation. Most gamma rays are emitted by the radioactive isotope,  $^{40}\text{K}$ , and by the radioactive elements of the U and Th series. The gamma-ray radiation originating in the formation close to the borehole wall is measured by a scintillation detector mounted inside the tool. The detector is a sodium-iodide crystal (NaI). Measurements are analyzed by subdividing the entire incident gamma-ray spectrum into five discrete energy windows. The total counts recorded in each window, for a specified depth in the well, are processed at the surface to give the elemental abundances of K, U, and Th. The final outputs are the total gamma ray (SGR), a uranium-free gamma-ray measurement (CGR) (both in API units), and the concentrations of potassium (POTA, wt% or decimal fraction), thorium (THOR, ppm), and uranium (URAN, ppm). The vertical resolution of the log is about 46 cm.

Because radioactive elements tend to be most abundant in clay minerals, the gamma-ray curve is commonly used to estimate clay or shale contents. Rock matrices, however, do exist for which the radioactivity values range from moderate to extremely high as a result of the presence of volcanic ash, potassic feldspar, or other radioactive minerals.

### Mechanical Caliper Device

The MCD provides a measure of borehole diameter. The hole-diameter (HD) log is used to detect washouts or constrictions. Borehole diameter significantly affects many of the other logging measurements, and the hole diameter is an important factor in log correction routines. This caliper tool is subject to sticking when formation mud gets into its mechanical parts, which result in bimodal (fully open or nearly fully closed) readings. In contrast, the hole-diameter measurement produced by the HLDT is much more reliable. Consequently, during Leg 143 the MCD tool was used primarily to provide centralization and associated improved log quality for the sonic log, rather than to measure hole diameter.

### Lithodensity Tool

The HLDT uses a  $^{137}\text{Cs}$  gamma-ray source and measures the resulting flux at fixed distances from the source (Fig. 10A). Under normal operating conditions, attenuation of gamma rays is caused chiefly by Compton scattering (Dewan, 1983). Formation density (RHOB) is extrapolated from this energy flux by assuming that the atomic weight of most rock-forming elements is approximately twice the atomic number. A photoelectric-effect index (PEF) also is provided. Photoelectric absorption occurs in the energy window below 150 keV and depends on the energy of the incident gamma rays, the atomic cross section, and the nature of the atom. Because this measurement is almost independent of porosity, it can be used directly as an indicator of matrix lithology. The radioactive source and detector array is placed in a tool that is pressed against the borehole wall by a strong spring arm; the position of this spring arm relative to the tool indicates hole diameter. Excessive roughness of the hole will cause some drilling fluid to infiltrate between the detector and the formation. As a consequence, density readings can be artificially low. Approximate corrections can be applied by using caliper data. The vertical resolution is about 38 cm.

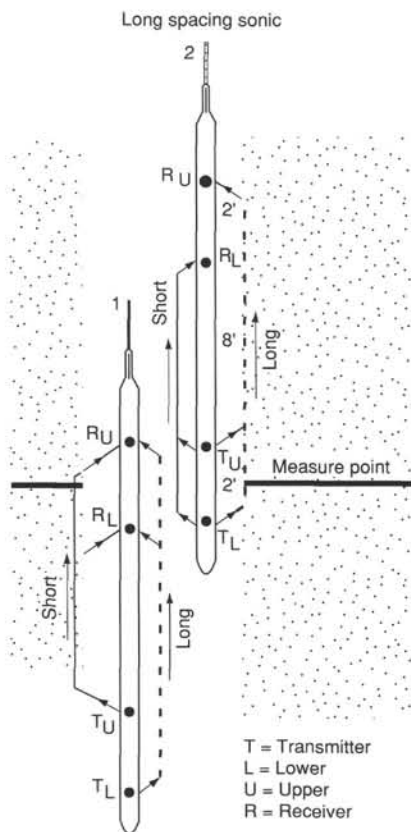


Figure 9. Sketch of Schlumberger acoustic tool (LSS).

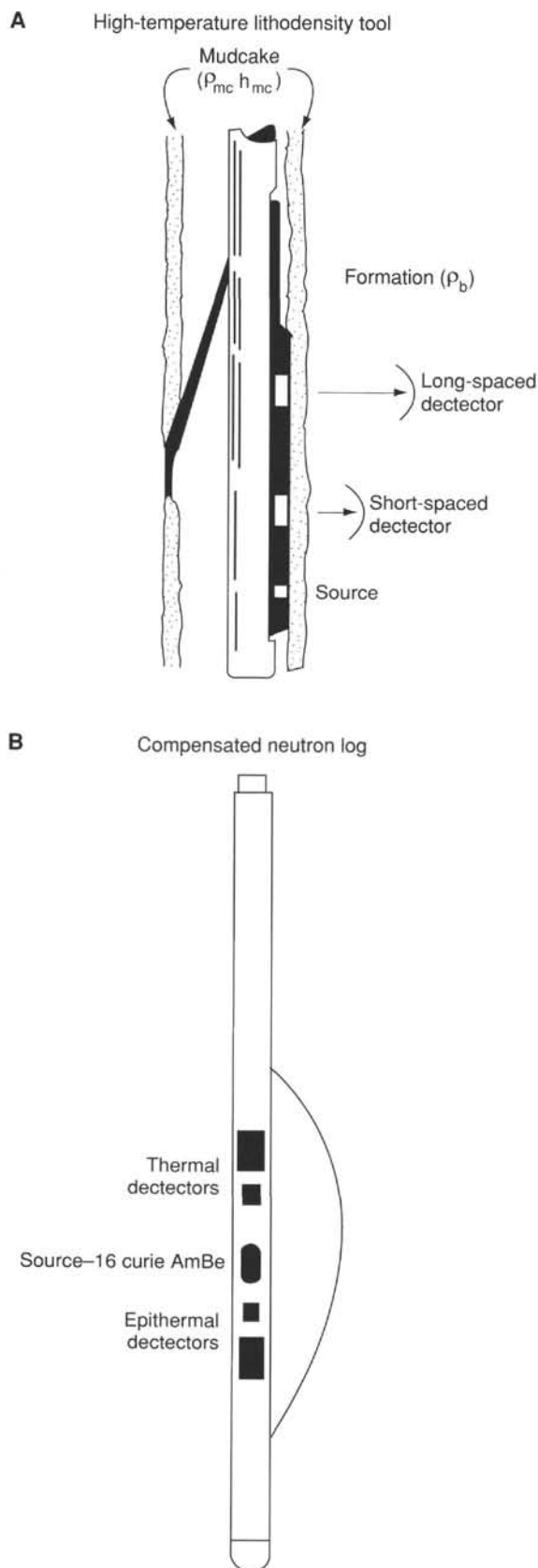


Figure 10. Schematic drawing of Schlumberger tools. **A.** HLDT. **B.** Porosity (CNT-G) tools.

### Gamma-Spectrometry Tool

The GST consists of a pulsed source of 14-MeV neutrons and a gamma-ray scintillation detector. A shipboard computer performs spectral analysis of gamma rays generated by the interactions of neutrons emitted by the source with atomic nuclei in the formation (Hertzog, 1979). Characteristic sets of gamma rays from six elements dominate the spectrum, permitting calculation of six elemental yields: calcium, silicon, iron, chlorine, hydrogen, and sulfur. The tool normalizes their sum, so that the yields do not reflect the actual elemental composition. Instead, ratios of these elemental yields are commonly used for interpreting the lithology, porosity, and salinity of the formation fluid. Shore-based processing is used to compute new elemental yields, and absolute dry-weight fractions of the major oxides.

### Aluminum Clay Tool

Aluminum abundance (as measured by the ACT) is determined by neutron-induced, gamma-ray spectrometry using californium ( $\text{Ca } 252$ ) as the chemical source. By placing NaI detectors (NGT tools) both above and below the neutron source, contributions from natural gamma-ray activity can be removed.

Calibration to elemental weight percent is performed by taking irradiated core samples of known volume and density and then measuring their gamma-ray output while placed in a jig attached to the logging tool (generally after logging).

### Formation Microscanner

The FMS produces high-resolution microresistivity images of the borehole wall that can be used for detailed sedimentological or structural interpretations and for determining fracture and breakout orientations. The tool (Fig. 11) consists of 16 electrodes, or "buttons," on each of four orthogonal pads that press against the borehole wall. The electrodes are spaced about 2.5 mm apart and are arranged in two diagonally offset rows of eight electrodes each. The focused current that flows from the buttons is recorded as a series of curves that reflect the microresistivity variations of the formation. Shipboard or shore-based processing converts the measurements into complete, spatially oriented images of the borehole wall. Further processing can provide measurements of dip and direction or azimuth of planar features. The vertical resolution of the FMS is about 1 cm, but coverage is restricted to about 22% of the borehole wall for each pass of the tool.

Applications of the FMS images include detailed correlation of coring and logging depths; orientation of cores; mapping of fractures, faults, foliations, and formation structures; as well as determining strikes and dips of bedding. The FMS can also be used to measure in-situ stress using breakout locations. In an isotropic, linearly elastic rock that has been subjected to an isotropic stress field, breakouts form in the direction of the least principal horizontal stress. Bell and Gough (1979) and Zoback et al. (1988) demonstrated that the stress orientations deduced from such rock breakouts are consistent with other independent stress indicators. An important limitation of the tool is the restriction of hole diameter to less than 40.6 cm (16.0 in.). Thus, no useful information can be obtained from washed-out hole sections.

### General Purpose Inclinator Tool (GPIT)

This tool provides a measurement of borehole inclination, the orientation of the tool with respect to Earth's magnetic field using a three-component magnetometer, and tool motion using an accelerometer. It is run with the FMS to provide spatial orientation for the borehole wall images.

### Borehole Televiwer

The borehole televiwer (BHTV) is a tool that produces an ultrasonic acoustical image of the borehole wall. A transducer emits

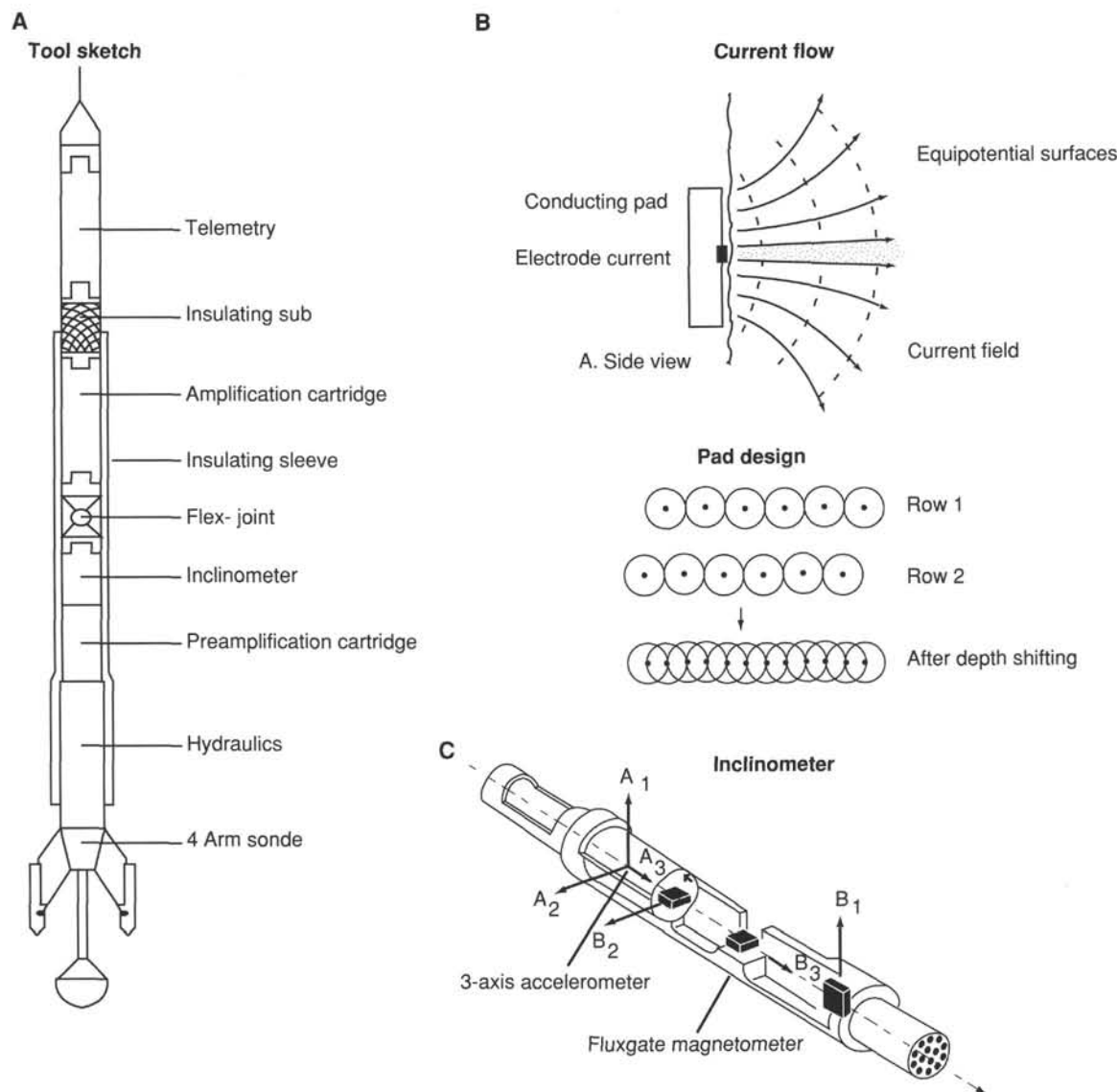


Figure 11. Sketches of the four-pad FMS sonde (A), current flow (B), pad configuration, and inclinometer (C) used for image orientation and correction of speed.

ultrasonic pulses that are reflected at the borehole wall and then are received by the same transducer. The amplitude and traveltime of the reflected signal are determined and stored. The 360° rotation of the transducer and the upward motion of the tool produce a complete map of the borehole wall.

The amplitude of the reflected signal depends on the reflection coefficient of the borehole fluid rock interface, the position of the BHTV tool in the borehole (it should be centered), the shape of the borehole, and the roughness of the borehole wall. The change of the roughness of the borehole wall (e.g., at fractures intersecting the borehole) is responsible for the amplitude modulation of the reflected signal. Thus, fractures or changes in character of the drilled rocks can be recognized easily in the amplitude image. Furthermore, the recorded traveltimes give detailed information about the shape of the borehole; knowing the velocity of the ultrasonic signal in the borehole fluid allows one to calculate the distance from the tool center to the wall (a "caliper" value) from each recorded traveltime. Typically, 128 points are recorded per transducer revolution, therefore the BHTV can be considered a "multi-arm caliper log."

Amplitude and traveltime are recorded together with reference to magnetic north, which permits proper data orientation. The BHTV then can be used to orient cores where structures in the core (e.g., fractures) are recognizable in the BHTV data.

### Downhole Three-component Magnetometer

This downhole magnetometer was designed and fabricated in Japan for downhole measurements in ODP holes. The magnetometer is composed of four high-pressure vessel sections, which are made of MONEL alloy and which house the measuring units. This nonmagnetic MONEL alloy (magnetic permeability is 1.001) has a high tensile strength at high temperature (no deterioration of strength up to 650°C). The thin, cylindrical magnetometer is 4.6 m long and 6.7 cm wide, which enables one to use it in almost all DSDP and ODP holes. Figure 12 shows a schematic drawing of the magnetometer. For ease of transport, the pressure vessel is separated into four 1.2-m sections. To operate as a downhole magnetometer, these four sections are connected into one long cylinder. A water-tight seal is attained

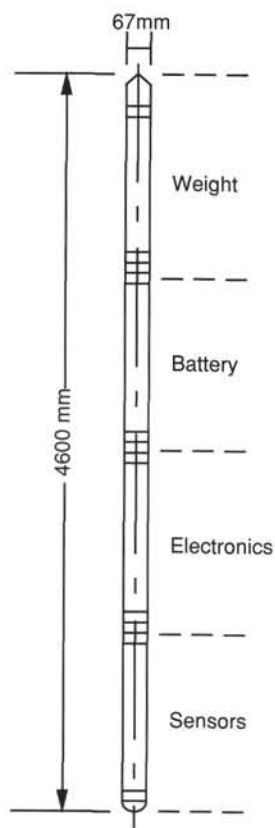


Figure 12. Schematic drawing of the Japanese downhole magnetometer.

using rubber O-rings. The total weight of the magnetometer tool is about 100 kg.

This tool measures temperature and the three orthogonal components of the magnetic field. A block diagram of the system is shown in Figure 13. Ring-core, fluxgate-type magnetic sensors are used for detecting the magnetic field. Three mutually perpendicular ring cores, drive coils, and pick-up coils are installed in the bottom section of the magnetometer. A semiconductor sensor (AD590) is used as a temperature sensor. These sensors are installed near the lower end of the bottom section.

The second section of the magnetometer houses the fluxgate magnetometer and temperature electronics, analog-to-digital (A/D) converters, and integrated-circuit (IC) memory. The fluxgate magnetometer electronics consist of the driving and the detection circuitry for the magnetic sensor. The driving frequency of the fluxgate sensor is 15 kHz, and the detection circuit converts the amplitude of higher harmonics, which is proportional to the external field strength in the sensor detection, to the direct-current (DC) output voltage. Sixteen-bit A/D converters are used by the three magnetic sensors and the temperature sensor. The digital data signals from the A/D converters are stored in IC memory, which consists of electrically programmable read-only memory (EEPROM). The maximum available memory space is 2048-kbit.

The third section contains a battery power source for the magnetometer. Seven batteries (National BR-C) are used to supply a voltage of  $\pm 18$  V. The top section contains lead weight, which increases the total mass for deployment purposes.

Besides the magnetometer, a shipboard controller box provides external power to check the magnetometer and transmits control signals to the magnetometer. It also contains an interface for the transfer of data from the magnetometer to a microcomputer for permanent storage. An NEC PC-9801 compatible computer is used as a host computer.

Resolution of the magnetic field is changeable; settings are 1.02, 1.36, and 2.03 nT. These resolution settings were calibrated by a Helmholtz coil at the Kakioka Magnetic Observatory. The measurement range of the magnetic field of each axis of the magnetometer is  $\pm 66519$  nT for lower resolution. Sampling interval is 3 s and maximum operation time is 12 h.

### Quality of Log Data

The quality of log data may be seriously degraded by excessively wide sections of the borehole or by rapid changes in the hole diameter. Resistivity and velocity measurements are least sensitive to borehole effects, whereas the nuclear measurements (density, neutron porosity, and both natural and induced spectral gamma ray) are most sensitive because of the large attenuation by the borehole fluid. Corrections can be applied to the original data to reduce the effects of these conditions and, generally, any departure from the conditions under which the tool was calibrated.

Logs from different tool strings may have small depth mismatches, caused by either cable stretch or ship-heave during recording. Small errors in depth-matching can impair the results in zones of rapidly varying lithology. To minimize the effects of ship-heave, a hydraulic heave compensator adjusts for rig motion during logging operations. Precise depth-matching of logs with cores is difficult in zones where core recovery is low because of the inherent ambiguity of placing the recovered section within the cored interval.

### Log Analysis

During logging, incoming data are observed on a monitor oscilloscope and simultaneously recorded on digital tape in the Schlumberger logging unit (CSU). After logging, the Schlumberger tape is read by computer in the downhole measurements laboratory and reformatted to a file format compatible with the Terralog log-interpretation software package. Most log interpretation (except geochemical log analysis) is performed aboard the ship; further analysis and interpretation are undertaken after the cruise at the Borehole Research Laboratory of Lamont-Doherty Geological Observatory.

### Synthetic Seismograms

Synthetic seismograms are generated from logging velocity data obtained using the LSS tool. The bulk density log from the LDT or a pseudodensity log created from other logs is required in addition to the sonic log. In many cases, a simple constant density log can be assumed. Experience shows that this often gives surprisingly good results, because both velocity and density are usually controlled by the same parameter: porosity. When velocity and density are highly correlated, synthetic seismograms using either a constant density log or an actual density log are virtually identical.

The slowness and density logs are used in a program that generates an impedance log (velocity density), which is convolved with a zero-phase Ricker or other assumed wavelet. The frequency of this wavelet can be varied, depending on the source that generated the original seismic profile. A 30-Hz wavelet is capable of a vertical resolution on the order of 30 m; thus, reflectors cannot generally be attributed to any small-scale lithologic horizons. The synthetic seismogram is calculated based on a convolutional model, with interbed multiples.

### REFERENCES\*

- Archie, G.E., 1942. The electrical resistivity log as an aid in determining some reservoir characteristics. *J. Pet. Tech.*, 5:1-8.
- ASTM, 1989. *Annual Book of ASTM Standards for Soil and Rock; Building Stones: Geotextiles* (Vol. 04.08): Philadelphia (ASTM), 168-862.
- Bates, R.G., and Calais, J.G., 1981. Thermodynamics of the dissociation of Bis.  $H^+$  in sea water from 5° to 40°C. *J. Solution Chem.*, 10:269-279.

- Bates, R.G., and Culberson, C.H., 1977. Hydrogen ions and the thermodynamic state of marine systems. In Anderson, N.R., and Malahoff, A. (Eds.), *The Fate of Fossil Fuel CO<sub>2</sub> in the Oceans*: New York (Plenum Press), 45–61.
- Bell, J.S., and Gough, D.I., 1979. Northeast-southwest compressive stress in Alberta: evidence from oil wells. *Earth Planet. Sci. Lett.*, 45:475–482.
- Berggren, W.A., Kent, D.V., and Flynn, J.J., 1985a. Jurassic to Paleogene: Part 2. Paleogene geochronology and chronostratigraphy. In Snelling, N.J. (Ed.), *The Chronology of the Geological Record*. Geol. Soc. London Mem., 10:141–195.
- Berggren, W.A., Kent, D.V., and Van Couvering, J.A., 1985b. The Neogene: Part 2. Neogene geochronology and chronostratigraphy. In Snelling, N.J. (Ed.), *The Chronology of the Geological Record*. Geol. Soc. London Mem., 10:211–260.
- Blow, W.H., 1969. Late middle Eocene to Recent planktonic foraminiferal biostratigraphy. In Brönniman, P., and Renz, H.H. (Eds.), *Proc. First Int. Conf. Planktonic Microfossils, Geneva, 1967*: Leiden (E. J. Brill), 1:199–422.
- Boyce, R.E., 1976. Definitions and laboratory techniques of compressional sound velocity parameters and wet-water content, wet-bulk density, and porosity parameters by gravimetric and gamma ray attenuation techniques. In Schlanger, S.O., Jackson, E.D., et al., *Init. Repts. DSDP*, 33: Washington (U.S. Govt. Printing Office), 931–958.
- Bralower, T.J., 1988. Calcareous nannofossil biostratigraphy and assemblages of the Cenomanian/Turonian boundary interval: implications for the origin and timing of oceanic anoxia. *Paleoceanography*, 8:275–316.
- Bralower, T.J., Sliter, W.V., Arthur, M.A., Leckie, R.M., Allard, D.J., and Schlanger, S.O., in press. Dysoxic/anoxic episodes in the Aptian/Albian (Early Cretaceous). In Pringle, M.S., Sager, W.W., Sliter, M.V., and Stein, S. (Eds.), *The Mesozoic Pacific*. Am. Geophys. Union. Monogr. Ser.
- Bukry, D., 1973. Low-latitude coccolith biostratigraphic zonation. In Edgar, N.T., Saunders, J.B., et al., *Init. Repts. DSDP*, 15: Washington (U.S. Govt. Printing Office), 685–703.
- Carlson, R.L., and Christensen, N.I., 1977. Velocity anisotropy and physical properties of deep-sea sediments from the western South Atlantic. In Perch-Nielsen, K., Supko, P.R., et al., *Init. Repts. DSDP*, 39: Washington (U.S. Govt. Printing Office), 555–559.
- Caron, M., 1985. Cretaceous planktic foraminifera. In Bolli, H.M., Saunders, J.B., and Perch-Nielsen, K. (Eds.), *Plankton Stratigraphy*: Cambridge (Cambridge Univ. Press), 17–86.
- Coogan, A., 1977. Early and middle Cretaceous Hippuritacea (Rudists) of the Gulf Coast. In Bebout, D.G., and Loucks, R.G. (Eds.), *Cretaceous Carbonates of Texas and Mexico: Applications to Subsurface Exploration*. Rep. Invest. - Univ. Tex. Austin, Bur. Econ. Geol., 89:32–70.
- Davies, P.J., McKenzie, J.A., Palmer-Julson, A., et al., 1991. *Proc. ODP, Init. Repts.*, 133: College Station, TX (Ocean Drilling Program).
- Deschaseaux, C., Coogan, A.H., Cox, L.R., and Perkins, B.F., 1969. In Moore, R.C. (Ed.), *Treatise on Invertebrate Paleontology* (Pt. N): *Mollusca 6 (Bivalvia)* (Vol. 2): Lawrence, KS (Geol. Soc. Am. and Univ. of Kansas), N776–N817.
- Dewan, J.T., 1983. *Essentials of Modern Open Hole Log Interpretation*: Tulsa (PennWell).
- Dunham, R., 1962. Classification of carbonate rocks according to depositional texture. In Ham, W.E. (Ed.), *Classification of Carbonate Rocks*. AAPG, 108–121.
- Embry, A.F., and Klovan, J.E., 1971. A late Devonian reef tract on northeastern Banks Island, Northwest Territories. *Bull. Can. Pet. Geol.*, 19:730–781.
- Emeis, K.-C., and Kvenvolden, K.A., 1986. Shipboard organic geochemistry on JOIDES Resolution. *ODP Tech. Note*, 7.
- Espitalié, J., Deroo, G., and Marquis, F., 1985. La pyrolyse Rock-Eval et ses applications. *Rev. Inst. Fr. Pet.*, 40/5:563–579; 40/6:755–784.
- , 1986. La pyrolyse Rock-Eval et ses applications. *Rev. Inst. Fr. Pet.*, 41/1:73–89.
- Espitalié, J., Laporte, J.L., Leplat, P., Madec, M., Marquis, F., Paulet, J., and Boutefeu, A., 1977. Méthode rapide de caractérisation des roches mères, de leur potentiel pétrolier et de leur degré d'évolution. *Rev. Inst. Fr. Pet.*, 32:23–42.
- Fisher, R.V., and Schmincke, H.-U., 1984. *Pyroclastic Rocks*: New York (Springer-Verlag).
- Gealy, E.L., Winterer, E.L., and Moberly, R., Jr., 1971. Methods, conventions, and general observations. In Winterer, E.L., Riedel, W.R., et al., *Init. Repts. DSDP*, 7 (Pt. 1): Washington (U.S. Govt. Printing Office), 9–26.
- Gieskes, J.M., 1973. Interstitial water studies, Leg 15: alkalinity, pH, Mg, Ca, Si, PO<sub>4</sub>, and NH<sub>4</sub>. In Heezen, B.C., MacGregor, I.D., et al., *Init. Repts. DSDP*, 20: Washington (U.S. Govt. Printing Office), 813–829.
- Gieskes, J.M., Gamo, T., and Brumsack, H.J., 1991. Chemical methods for interstitial water analysis on JOIDES Resolution. *ODP Tech. Note*, 15.
- Harland, W.B., Armstrong, R.L., Cox, A.V., Craig, L.E., Smith, A.G., and Smith, D.G., 1990. *A Geological Time Scale 1989*: Cambridge (Cambridge Univ. Press).
- Hertzog, R., 1979. Laboratory and field evaluation of an inelastic-neutron-scattering and capture gamma-ray spectroscopy tool. *Soc. Pet. Eng. Pap.*, 7430.
- Jaeger, J.C., 1961. The effect of the drilling fluid on temperatures measured in boreholes. *J. Geophys. Res.*, 66:563–569.
- Kennett, J.P., and Srinivasan, M.S., 1983. *Neogene Planktonic Foraminifera: A Phylogenetic Atlas*: Stroudsburg, PA (Hutchinson Ross).
- Kent, D.V., and Gradstein, F.M., 1985. A Cretaceous and Jurassic geochronology. *Geol. Soc. Am. Bull.*, 96:1419–1427.
- Kvenvolden, K.A., and McDonald, T.J., 1986. Organic geochemistry on the JOIDES Resolution—an assay. *ODP Tech. Note*, 6.
- Lewis, D.W., 1984. *Practical Sedimentology*: New York (Van Nostrand-Reinhold).
- Mahoney, J., Story, M., Duncan, R.A., Spencer, K.J., and Pringle, M., in press. Geochemistry and geochronology of Leg 130 basement lavas: nature and origin of the Ontong Java Plateau. In Berger, W.H., Kroenke, L.W., Mayer, L.A., et al., *Proc. ODP, Sci. Results*, 130: College Station, TX (Ocean Drilling Program).
- Manheim, F.T., and Sayles, F.L., 1974. Composition and origin of interstitial waters of marine sediments based on deep sea drill cores. In Goldberg, E.D. (Ed.), *The Sea* (Vol. 5): New York (Wiley Interscience), 527–568.
- Martini, E., 1971. Standard Tertiary and Quaternary calcareous nannoplankton zonation. In Farinacci, A. (Ed.), *Proc. 2nd Int. Conf. Planktonic Microfossils Roma*: Rome (Ed. Tecnosci.), 2:739–785.
- Matthews, D.J., 1939. *Tables of Velocity of Sound in Pore Water and in Seawater*: London (Admiralty, Hydrogr. Dept.).
- Mazzullo, J.M., Meyer, A., and Kidd, R., 1987. New sediment classification scheme for the Ocean Drilling Program. In Mazzullo, J., and Graham, A.G. (Eds.), *Handbook for Shipboard Sedimentologists*. ODP Tech. Note, 8:45–67.
- Monechi, S., and Thierstein, H.R., 1985. Late Cretaceous-Eocene nannofossil and magnetostratigraphic correlations near Gubbio, Italy. *Mar. Micropaleontol.*, 9:419–440.
- Munsell Soil Color Charts, 1971. Baltimore, MD (Munsell Color).
- Mutterlose, J., in press. Biostratigraphy and palaeobiogeography of Early Cretaceous calcareous nannofossils. *Cretaceous Res.*
- Norris, K., and Hutton, J.T., 1969. An accurate X-ray spectrographic method for the analysis of a wide range of geological samples. *Geochim. Cosmochim. Acta*, 33:431–453.
- Perch-Nielsen, K., 1985. Mesozoic calcareous nannofossils. In Bolli, H.M., Saunders, J.B., and Perch-Nielsen, K. (Eds.), *Plankton Stratigraphy*: Cambridge (Cambridge Univ. Press), 329–426.
- Reynolds, R.C., 1967. Estimations of mass absorption coefficients by Compton scattering: improvements and extensions of the method. *Am. Mineral.*, 48:1133–1143.
- Roth, P.H., 1978. Cretaceous nannoplankton biostratigraphy and oceanography of the northwestern Atlantic Ocean. In Benson, W.E., Sheridan, R.E., et al., *Init. Repts. DSDP*, 44: Washington (U.S. Govt. Printing Office), 731–760.
- Roth, P.H., and Thierstein, H.R., 1972. Calcareous nannoplankton: Leg 14 of the Deep Sea Drilling Project. In Hayes, D.E., Pimm, A.C., et al., *Init. Repts. DSDP*, 14: Washington (U.S. Govt. Printing Office), 421–485.
- Schlager, W., and James, N.P., 1978. Low-magnesian calcite limestones forming at the deep-sea floor, Tongue of the Ocean, Bahamas. *Sedimentology*, 25:675–702.
- Schlumberger, Inc., 1972. *Log Interpretation* (Vol. 1): New York (Schlumberger).
- Serra, O., 1984. *Fundamentals of Well Log Interpretation* (Vol. 1): *The Acquisition of Logging Data*: Amsterdam (Elsevier).
- Shepard, F., 1954. Nomenclature based on sand-silt-clay ratios. *J. Sediment. Petrol.*, 24:151–158.
- Sissingh, W., 1977. Biostratigraphy of Cretaceous calcareous nannoplankton. *Geol. Mijnbouw*, 56:37–65.
- Skelton, P., 1982. Aptian and Barremian rudist bivalves of the New World: some old world similarities. *Cretaceous Res.*, 3:145–153.
- Sliter, W.V., 1986. Cretaceous redeposited benthic foraminifers from Deep Sea Drilling Project Site 585 in the East Mariana Basin, western equatorial Pacific, and implications for the geologic history of the region. In Moberly, R., Schlanger, S.O., et al., *Init. Repts. DSDP*, 89: Washington (U.S. Govt. Printing Office), 327–361.

- Sliter, W.V., 1989. Biostratigraphic zonation for Cretaceous planktonic foraminifers examined in thin section. *J. Foraminiferal Res.*, 19:1–19.
- Solorzano, L., 1969. Determination of ammonia in natural waters by phenol-hypochlorite method. *Limnol. Oceanogr.*, 14:799–801.
- Strickland, J.D.H., and Parsons, T.R., 1968. A manual for seawater analysis. *Bull. Fish. Res. Bd. Can.*, 167:311.
- Tarduno, J., Sliter, W.V., Bralower, T.J., McWilliams, M., Premoli Silva, I., and Ogg, J.G., 1989. M-sequence reversals recorded in DSDP sediment cores from the western Mid-Pacific Mountains and Magellan Rise. *Geol. Soc. Am. Bull.*, 101:1306–1316.
- Tarduno, J.A., Mayer, L.A., Musgrave, R., and Shipboard Scientific Party, 1991a. High-resolution, whole-core magnetic susceptibility data from Leg 130, Ontong Java Plateau. In Kroenke, L.W., Berger, W.H., Janecek, T.R., et al., *Proc. ODP, Init. Repts.*, 130: College Station, TX (Ocean Drilling Program), 541–548.
- Tarduno, J.A., Sliter, W.V., Kroenke, L., Leckie, M., Mayer, H., Mahoney, J.J., Musgrave, R., Storey, M., and Winterer, E.L., 1991b. Rapid formation of Ontong Java Plateau by Aptian mantle plume volcanism. *Science*, 254:399–403.
- Thierstein, H.R., 1971. Tentative Lower Cretaceous calcareous nannoplankton zonation. *Eclogae Geol. Helv.*, 64:458–488.
- , 1973. Lower Cretaceous calcareous nannoplankton biostratigraphy. *Abh. Geol. Bundesanst. (Austria)*, 29:1–52.
- Timur, A., and Toksöz, M.N., 1985. Downhole geophysical logging. *Annu. Rev. Earth Planet. Sci.*, 14:315–344.
- Tsunogai, S., Nishimura, M., and Nakaya, S., 1968. Complete metric titration of calcium in the presence of large amounts of magnesium. *Talanta*, 15:385–390.
- Vacquier, V., 1985. The measurement of thermal conductivity of solids with a transient linear heat source on the plane surface of a poorly conducting body. *Earth Planet. Sci. Lett.*, 74:275–279.
- Von Herzen, R.P., and Maxwell, A.E., 1959. The measurement of thermal conductivity of deep-sea sediments by a needle probe method. *J. Geophys. Res.*, 65:1557–1563.
- Wentworth, C.K., 1922. A scale of grade and class terms of clastic sediments. *J. Geol.*, 30:377–392.
- Zoback, M.D., Zoback, M.L., Mount, V.S., Suppe, J., Eaton, J.P., Healy, J.H., Oppenheimer, D., Reasenber, P., Jones, L., Raleigh, C.B., Wong, I.G., Scotti, O., and Wentworth, C., 1988. New evidence on the state of stress of the San Andreas Fault. *Science*, 238:1105–1111.

\* Abbreviations for names of organizations and publication titles in ODP reference lists follow the style given in *Chemical Abstracts Service Source Index* (published by American Chemical Society).

Ms 143IR-105

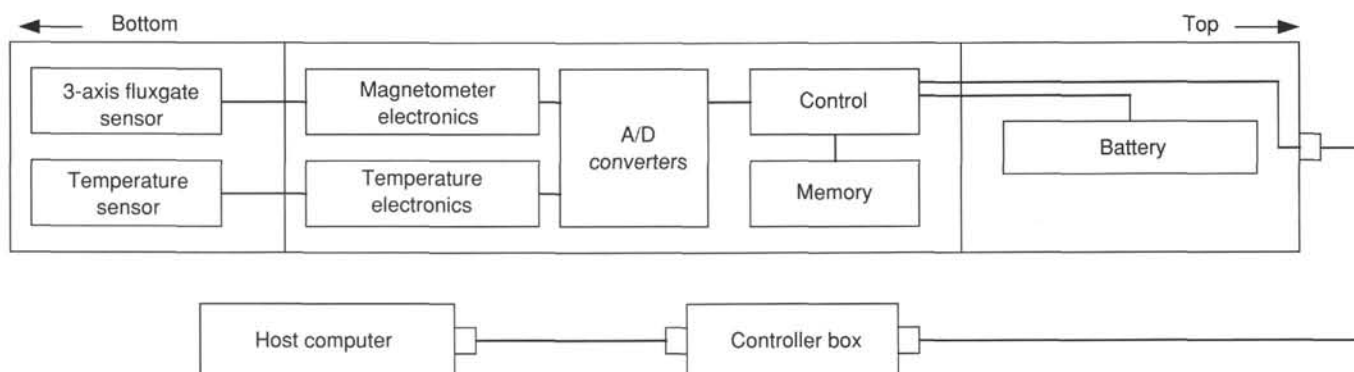


Figure 13. Downhole magnetometer system in block-diagram form.